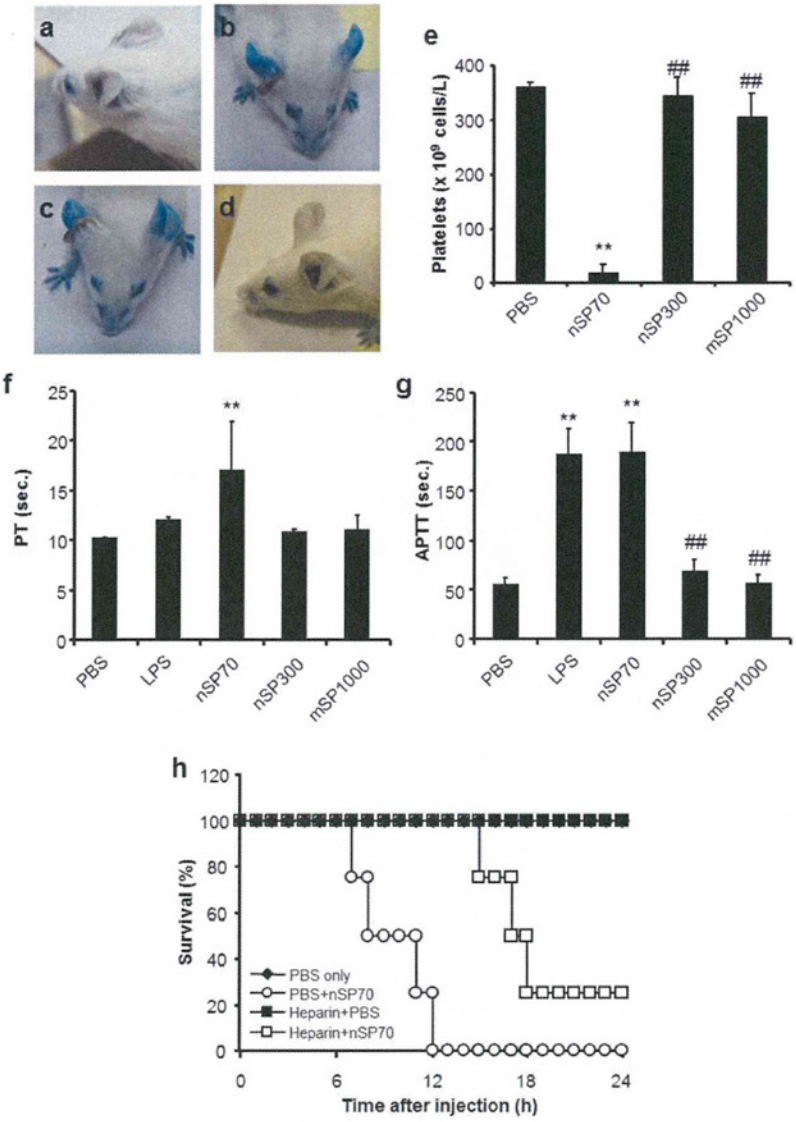

Figure 4. Blood coagulation analysis in mice injected with silica particles. (a)–(d) Influence of nSPs on microvascular leakage in BALB/c mouse skin. Photograph of mouse treated with PBS (a), nSP70 (b), nSP100 (c), or nSP300 (d) 90 min after treatment. Evans Blue extravasations were observed only in nSP70 and nSP100-treated mice. (e) Hematology analysis in whole blood of mice injected with silica particles. Blood samples from BALB/c mice injected intravenously with 100 mg kg^{-1} silica particles (nSP70, 300, and mSP1000) or PBS (control) were collected from heart 5 h after injection. Hematology analysis was performed using VetScan. Results are expressed as mean ± S.E. ($n = 3$). (f), (g) Coagulation response of the plasma of silica particle-injected mice. Plasma samples were collected from BALB/c mice injected with 100 mg kg^{-1} silica particles (nSP70, 300, and mSP1000), LPS (positive control), or PBS (control) 5 h after injection. Plasma was then assayed for PT (f) and APTT (g) by standard methods. Results are expressed as mean ± S.E. ($n = 3$). (h) The protective effect of anticoagulant on nSP70-induced lethal toxicity. 100 IU/mouse heparin or PBS (vehicle) was administrated by intravenous injection 2 min before nSP70 or PBS (control) injection. Survival was monitored for 24 h after injection. ** represents significant difference from the control ($P < 0.01$), ## represents significant difference from the nSP70 group ($P < 0.01$).

size was the same [31]. Although the mechanism of this finding is unclear, we speculate that one of the mechanisms is the change of interaction between nSPs and biological molecules such as protein induced by the surface properties of nSPs. Therefore, our current studies focus on analyzing biological interactions that nanoparticles may encounter in tissue culture medium, and following the interactions with cells (membranes, endosomes, organelles, and cytoplasm) or concomitantly administered drugs and foods.

4. Conclusions

We reveal here that the emergence of acute toxicity of nSPs would be dependent on both particle size and material effect such as the difference of blood coagulation activity and distribution behavior. These results suggest the importance of risk management of nSPs and the need for more information of nSPs' safety. We are now examining in detail the biological responses, biodistribution, and biological interactions which

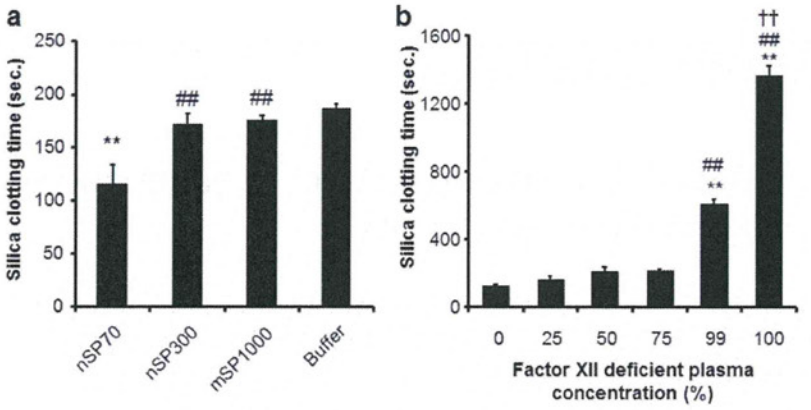

Figure 5. Measurement of the blood clotting time and the factor XII activation rate by silica particles *in vitro*. (a) Changes in silica clotting time with different sized silica particles (0.02 mg ml^{-1}) in healthy human plasma. Results are expressed as mean ± S.D. ($n = 3$). ** represents a significant difference from the buffer group ($P < 0.01$), ## represents a significant difference from the nSP70 group ($P < 0.01$). (b) *In vitro* silica clotting time measurement using mixtures of healthy and factor XII-deficient human plasma in various proportions. Silica clotting time was measured with nSP70 (0.02 mg ml^{-1}) using normal healthy plasma mixed with different amounts of coagulant factor XII-deficient human plasma (0 (healthy human plasma alone), 25, 50, 75, 99, and 100% (coagulant factor XII-deficient human plasma alone)). Results are expressed as mean ± S.D. ($n = 3$). ** represents a significant difference from 0% factor XII-deficient human plasma ($P < 0.01$), ## represents a significant difference from 25, 50, and 75% factor XII-deficient human plasma ($P < 0.01$), †† represents a significant difference from 99% factor XII-deficient human plasma ($P < 0.01$).

are linked to the physicochemical properties of NMs. We believe that the knowledge obtained from this research may constitute useful information for ensuring the safety of NMs.

Acknowledgments

This study was supported in part by Grants-in-Aid for Scientific Research from the Ministry of Education, Culture, Sports, Science, and Technology of Japan (MEXT), the Japan Society for the Promotion of Science (JSPS), the Knowledge Cluster Initiative (MEXT), and by Health Labour Sciences Research Grants from the Ministry of Health, Labor, and Welfare of Japan (MHLW), by a Global Environment Research Fund from the Minister of the Environment, by the Food Safety Commission (Cabinet Office), by The Cosmetology Research Foundation, by The Smoking Research Foundation, and by The Takeda Science Foundation.

References

[1] Royal Commission on Environmental Pollution 2008 *Novel Materials in the Environment: the Case of Nanotechnology* (London: Royal Commission) www.official-documents.gov.uk/document/cm74/7468/7468.pdf
[2] Merget R, Bauer T, Kupper H U, Philippou S, Bauer H D, Breitstadt R and Bruening T 2002 *Arch. Toxicol.* **75** 625
[3] Evonik 2008 Evonik, Documents on Aerosil [online] www.aerosil.com/aerosil/en/industries/food/default www.aerosil.com/aerosil/en/industries/personalcare/skincare/default www.aerosil.com/aerosil/en/industries/personalcare/haircare/ www.aerosil.com/aerosil/en/industries/personalcare/cosmetic/
[4] Grobe A, Renn O and Jaeger A 2008 *Risk Governance of Nanotechnology Applications in Food and Cosmetics* (Geneva: International Risk Governance Council) www.irgc.org/IMG/pdf/IRGC_Report_FINAL_For_Web.pdf
[5] Bharali D J, Klejbor I, Stachowiak E K, Dutta P, Roy I, Kaur N, Bergey E J, Prasad P N and Stachowiak M K 2005 *Proc. Natl Acad. Sci. USA* A **102** 11539
[6] Bottini M *et al* 2007 *Int. J. Nanomed.* **2** 227
[7] Hirsch L R, Stafford R J, Bankson J A, Sershen S R, Rivera B, Price R E, Hazle J D, Halas N J and West J L 2003 *Proc. Natl Acad. Sci. USA* A **100** 13549
[8] Roy I, Ohulchanskyy T Y, Bharali D J, Pudavar H E, Mistretta R A, Kaur N and Prasad P N 2005 *Proc. Natl Acad. Sci. USA* A **102** 279
[9] Verraedt E, Pendela M, Adams E, Hoogmartens J and Martens J A 2010 *J. Control. Release* **142** 47
[10] Nabeshi H *et al* 2011 *Biomaterials* **32** 2713
[11] Yamashita K *et al* 2011 *Nature Nanotechnol.* **6** 321
[12] Nabeshi H *et al* 2011 *Part. Fibre Toxicol.* **8** 1
[13] Hardisty R M and Margolis J 1959 *Br. J. Haematol.* **5** 203
[14] Bloom A L 1962 *J. Clin. Pathol.* **15** 508
[15] Cochrane C G and Griffin J H 1982 *Adv. Immunol.* **33** 241
[16] Colman R W and Schmaier A H 1997 *Blood* **90** 3819
[17] Vogler E A, Graper J C, Harper G R, Sugg H W, Lander L M and Brittain W J 1995 *J. Biomed. Mater. Res.* **29** 1005
[18] Vogler E A, Graper J C, Sugg H W, Lander L M and Brittain W J 1995 *J. Biomed. Mater. Res.* **29** 1017
[19] Vogler E A, Nadeau J G and Graper J C 1998 *J. Biomed. Mater. Res.* **40** 92
[20] Zhuo R, Miller R, Bussard K M, Siedlecki C A and Vogler E A 2005 *Biomaterials* **26** 2965
[21] Borm P, Klaessig F C, Landry T D, Moudgil B, Pauluhn J, Thomas K, Trottier R and Wood S 2006 *Toxicol. Sci.* **90** 23
[22] Nel A, Xia T, Madler L and Li N 2006 *Science* **311** 622
[23] Xia T *et al* 2006 *Nano Lett.* **6** 179
[24] Rahman I A, Vejayakumaran P, Sipaut S C, Ismail J and Chee K C 2009 *Mater. Chem. Phys.* **114** 328
[25] Gorbet M B and Sefton M V 2004 *Biomaterials* **25** 5681
[26] Miller L L and Bale W F 1954 *J. Exp. Med.* **99** 125
[27] Miller L L, Bly C G, Watson M L and Bale W F 1951 *J. Exp. Med.* **94** 431
[28] Tennent G A, Brennan S O, Stangou A J, O'Grady J, Hawkins P N and Pepys M B 2007 *Blood* **109** 1971–4
[29] Gordon E M, Gallagher C A, Johnson T R, Blossey B K and Ilan J 1990 *J. Lab. Clin. Med.* **115** 463
[30] Tsuruta J, Yamamoto T and Kambara T 1986 *Adv. Exp. Med. Biol.* B **198** 63
[31] Nabeshi H *et al* 2011 *Nanosc. Res. Lett.* **6** 93

Arch Toxicol
DOI 10.1007/s00204-012-0823-5

INORGANIC COMPOUNDS

Suppression of nanosilica particle-induced inflammation by surface modification of the particles

Tomohiro Morishige · Yasuo Yoshioka · Hiroshi Inakura · Aya Tanabe · Shogo Narimatsu · Xinglei Yao · Youko Monobe · Takayoshi Imazawa · Shin-ichi Tsunoda · Yasuo Tsutsumi · Yohei Mukai · Naoki Okada · Shinsaku Nakagawa

Received: 17 August 2011 / Accepted: 27 February 2012

Abstract It has gradually become evident that nanomaterials, which are widely used in cosmetics, foods, and medicinal products, could induce substantial inflammation. However, the roles played by the physical characteristics of nanomaterials in inflammatory responses have not been elucidated. Here, we examined how particle size and surface modification influenced the inflammatory effects of nanosilica particles, and we investigated the mechanisms by which the particles induced inflammation. We compared the inflammatory effects of silica particles with diameters of 30–1,000 nm in vitro and in vivo. In macrophages in vitro, 30- and 70-nm nanosilica particles (nSP30 and nSP70) induced higher production of tumor necrosis factor-α (TNFα) than did larger particles. In addition, intraperitoneal injection of nSP30 and nSP70 induced stronger inflammatory responses involving cytokine production than did larger particles in mice. nSP70-induced TNFα production in macrophage depended on the production of reactive oxygen species and the activation of mitogen-activated protein kinases (MAPKs). Furthermore, nSP70-induced inflammatory responses were dramatically suppressed by surface modification of the particles with carboxyl groups in vitro and in vivo; the mechanism of the suppression involved reduction in MAPK activation. These results provide basic information that will be useful for the development of safe nanomaterials.

Keywords Inflammation · Macrophage · Nanoparticle · Silica · Surface modification

Abbreviations

BHA	Butylated hydroxyanisole
DPI	Diphenyleneiodonium chloride
ELISA	Enzyme-linked immunosorbent assay
ERK	Extracellular signal-regulated kinase
IL	Interleukin
JNK	C-jun N-terminal kinase
KC	Keratinocyte chemoattractant
MAPKs	Mitogen-activated protein kinases
MCP-1	Macrophage chemoattractant protein-1
PBS	Phosphate-buffered saline
PCLF	Peritoneal cavity lavage fluid
ROS	Reactive oxygen species
TEM	Transmission electron microscopy
TNFα	Tumor necrosis factor-α

T. Morishige · H. Inakura · A. Tanabe · S. Narimatsu · X. Yao · Y. Mukai · N. Okada · S. Nakagawa (✉)
Laboratory of Biotechnology and Therapeutics, Graduate School of Pharmaceutical Sciences, Osaka University, 1-6 Yamadaoka, Suita, Osaka 565-0871, Japan
e-mail: nakagawa@phs.osaka-u.ac.jp

Y. Yoshioka · S. Tsunoda · Y. Tsutsumi · S. Nakagawa
The Center for Advanced Medical Engineering and Informatics, Osaka University, 1-6 Yamadaoka, Suita, Osaka 565-0871, Japan

Y. Yoshioka · S. Tsunoda · Y. Tsutsumi
Laboratory of Biopharmaceutical Research, National Institute of Biomedical Innovation, Osaka 567-0085, Japan

X. Yao
Institute of Pharmaceutics, Zhejiang University, 388 Yuhangtang Road, Hangzhou 310058, China

Y. Monobe · T. Imazawa
Laboratory of Common Apparatus, Division of Biomedical Research, National Institute of Biomedical Innovation, Osaka 567-0085, Japan

Y. Tsutsumi
Laboratory of Toxicology and Safety Science, Graduate School of Pharmaceutical Sciences, Osaka University, Osaka 565-0871, Japan

Published online: 15 March 2012

Introduction

Many nanomaterials with innovative functions have been developed. For example, titanium dioxide nanoparticles, carbon nanotubes, and nanosilica particles have already been used commercially in electronics, medicine, cosmetics, and foods. Amorphous (noncrystalline) nanosilica particles with extraordinary properties can be synthesized by straightforward methods and are relatively inexpensive, and surface modification of the particles is easy to accomplish. In addition, they are usually considered to have low toxicity, in contrast to crystalline silica, which can cause silicosis and some forms of lung cancer (Huaux 2007; Mossman and Churg 1998). Therefore, nanosilica particles have been used for many applications, including cosmetics, foods, medical diagnosis, and drug delivery (Bharali et al. 2005; Bottini et al. 2007; Hirsch et al. 2003; Roy et al. 2005; Verraedt et al. 2009).

However, the increasing use of nanomaterials has raised public concern about their safety (Kagan et al. 2005; Nel et al. 2006). Carbon nanotubes have been reported to induce mesothelioma-like lesions in mice upon injection (Poland et al. 2008; Takagi et al. 2008), in a similar manner to crocidolite asbestos, and to suppress the immune system and damage DNA (Mitchell et al. 2009; Yamashita et al. 2010). Furthermore, nanosilica particles have been reported to induce oxidative stress, genotoxicity, and inflammation in vitro and in vivo (Chen et al. 2008; Liu and Sun 2010; Yang et al. 2010). Because inflammation has been implicated as the key factor in the development of chronic obstructive pulmonary disease, fibrosis, and carcinogenesis (Dostert et al. 2008; Mantovani et al. 2008), the need to investigate the inflammatory effects of nanosilica particles and ensure their safety is urgent.

Our group and others have recently reported that the characteristics of particles, including size and surface properties, are important factors in pathologic alterations and cellular responses (Albrecht et al. 2004; He et al. 2008; Morishige et al. 2010a, b; Waters et al. 2009; Yamashita et al. 2011). For example, we showed that administration of nanosilica particles into pregnant mice induces pregnancy complications, whereas microsilica particles have no effect (Yamashita et al. 2011). Furthermore, Decuzzi et al. (2010) demonstrated that the biodistribution of silica particles depends on particle size. However, only a few studies have assessed the roles of the physical characteristics of nanomaterials in relation to the inflammatory responses they induce. Therefore, the relationship between nanoparticle characteristics and biological effects, including inflammatory effects, and the precise mechanisms of these effects must be investigated. In addition, the results of such investigations should be used to develop a methodology for decreasing the adverse biological effects of nanomaterials.

In this study, we evaluated the correlation between inflammatory effects and the size and surface modification of silica particles. Furthermore, we investigated the mechanisms of the inflammatory responses induced by nanosilica particles.

Materials and methods

Materials and reagents

Unmodified amorphous silica particles with diameters of 30, 70, 300, or 1,000 nm (designated nSP30, nSP70, nSP300, and mSP1000, respectively) and nSP70 with surface carboxyl groups (nSP70-C) were purchased from Micromod Partikeltechnologie (Rostock/Warnemünde, Germany). Butylated hydroxyanisole (BHA) and diphenyleneiodonium chloride (DPI) were purchased from Sigma-Aldrich (St. Louis, MO). Rabbit polyclonal anti-phospho-p38 antibody (sc-17852-R) and mouse monoclonal anti-β-actin antibody (sc-47778; clone C4) were purchased from Santa Cruz Biotechnology (Santa Cruz, CA). Rabbit polyclonal anti-extracellular signal-regulated kinase (ERK)1/2 antibody (#9102), rabbit polyclonal anti-c-jun N-terminal kinase (JNK) antibody (#9252), rabbit monoclonal anti-phospho-JNK antibody (#4671; clone 98F2), and goat anti-rabbit peroxidase-conjugated antibody (#7074) were purchased from Cell Signaling Technology (Danvers, MA). Rabbit monoclonal anti-phospho-ERK1/2 antibody (MAB1018; clone269434) was obtained from R&D Systems (Minneapolis, MN). Rabbit polyclonal anti-p38 antibody (ab47437) was purchased from Abcam (Tokyo, Japan). Goat anti-mouse peroxidase-conjugated antibody was purchased from SouthernBiotech (Birmingham, AL). p38 inhibitor SB203580, ERK inhibitor U0126, and JNK inhibitor SP600125 were obtained from Merck (Darmstadt, Germany).

Cells and mice

RAW264.7 (mouse monocyte/macrophage cell line) cells were obtained from the American Type Culture Collection (Manassas, VA) and cultured at 37°C in Dulbecco's modified Eagle's medium (Wako Pure Chemical Industries, Osaka, Japan) supplemented with 10% fetal bovine serum and antibiotics. Female BALB/c mice were purchased from Nippon SLC (Shizuoka, Japan) and used at 8 weeks of age. All the animal experimental procedures were performed in accordance with Osaka University's guidelines for the welfare of animals.

Silica particle characterization

The size distributions of the silica particles were measured with a Zetasizer 3000HS (Worcestershire, United Kingdom) after sonication of the particles at a concentration of 300 μg/mL in H_2O.

Cytotoxicity assay and cytokine production assay

RAW264.7 cells (1.5×10^4 cells/well) were seeded in 96-well plates (Nunc, Rochester, NY), cultured at 37°C for 12 h, and then treated with each type of silica particle (100 μg/mL) or medium (for negative control) for 12 h. The cytotoxicity of the silica particles was assessed by means of the standard methylene blue assay method, as previously described (Morishige et al. 2010a). Production of tumor necrosis factor-α (TNFα) in culture supernatants was assessed by means of an enzyme-linked immunosorbent assay (ELISA) kit (BD Pharmingen, San Diego, CA) according to the manufacturer's instructions.

Inhibitory assay

RAW264.7 cells (1.5×10^4 cells/well) were seeded in 96-well plates (Nunc), cultured at 37°C for 12 h, and then preincubated for 2 h with SB203580 (50 μM), U0126 (50 μM), SP600125 (10 μM), BHA (50 or 250 μM), or DPI (2 or 10 μM). Then, the cells were treated with one type of silica particle (100 μg/mL) or medium (for negative control) for 4 h. TNFα production in the culture supernatants was assessed by means of an ELISA kit (BD Pharmingen) according to the manufacturer's instructions.

Western blotting analysis

RAW264.7 cells were seeded in 12-well plates, cultured at 37°C for 12 h, and then treated with one type of silica particle (100 μg/mL) or medium (for negative control) for 0.5, 1, 2, or 4 h. For positive control, cells were treated with lipopolysaccharide (LPS) (1.25 μg/mL) for 30 min. Cells were then washed with PBS and lysed with Mammalian Protein Extraction Reagent (M-PER; Thermo Fisher Scientific, Rockford, IL) containing a Halt Protease Inhibitor Cocktail Kit (Thermo Fisher Scientific) and Phosphatase Inhibitor Cocktail (Nacalai Tesque, Kyoto, Japan). Then protein samples (1–5 μg) were loaded on a 20% sodium dodecyl sulfate–polyacrylamide gel. After electrophoresis, proteins were transferred to polyvinylidene difluoride membranes (GE Healthcare, Buckinghamshire, United Kingdom). The blots were blocked with 4% ECL Advance Blocking Agent (GE Healthcare) in TBS/T buffer (20 mM Tris–HCl [pH 7.6], 137 mM NaCl, 0.1% Tween 20) for 2 h at room temperature. The blots were washed with TBS/T and incubated with primary antibodies overnight at 4°C. Goat anti-rabbit or goat anti-mouse peroxidase-conjugated secondary antibody was added to the membranes, which were then incubated for 1 h at room temperature. The protein bands on the membrane were visualized with SuperSignal West Femto Maximum Sensitivity Substrate (Thermo Fisher Scientific).

Transmission electron microscopy (TEM) analysis

RAW264.7 cells (3×10^5 cells/well) were seeded in 4-well Lab-Tek II Chambered Coverglass (Nunc), cultured at 37°C for 6 h, treated with 100 μg/mL nSP70, nSP70-C or medium (for negative control), and fixed in 2.5% glutaraldehyde and then in 1.5% osmium tetraoxide. The fixed cells were dehydrated and embedded in EPON resin. Ultrathin sections were stained with lead citrate and observed by transmission electron microscopy (HITACHI-H7650, HITACHI, Tokyo, Japan).

Assessment of in vivo inflammatory effects of silica particles

BALB/c mice were intraperitoneally injected with 1 mg of one type of silica particle in 200 μL phosphate-buffered saline (PBS) or PBS for negative control. Two or twenty-four hours after injection, the mice were sacrificed, and whole peritoneal cavity lavage fluid (PCLF) was collected using 4 mL of cooled PBS as previously described (Kops et al. 1986; Morishige et al. 2010a). Cytokine production patterns in the PCLF 2 h after injection were analyzed by means of a Mouse Cytokine 20-Plex Panel (Invitrogen, Carlsbad, CA) using a Bio-Plex Suspension Array System (Bio-Rad Laboratories, Tokyo, Japan). The total number of live cells in the PCLF 24 h after injection was determined with a Nucleo-Counter (Chemometec A/S, Allerød, Denmark).

Statistical analysis

All results are presented as means ± standard deviation (SD) or standard error of the mean (SEM). Differences were compared by using Student's *t*-tests or Scheffé's method after analysis of variance (ANOVA).

Results

Size dependence of silica particle-induced inflammatory responses

Here, we used nanosilica particles with diameters of 30 and 70 nm (nSP30 and nSP70, respectively) and conventional

microsilica particles with diameters of 300 and 1,000 nm (nSP300 and mSP1000, respectively). The hydrodynamic diameters of these particles, as measured by means of a dynamic light-scattering system, were 33, 78, 300, and 945 nm, respectively (Fig. 1a). The size distribution spectrum of each silica particle showed a single peak (Fig. 1a), and the hydrodynamic diameter corresponded almost precisely to the primary particle size for each sample, indicating that the silica particles used in this study were well-dispersed particles in solution. In addition, TEM images confirmed that the particles were well-dispersed smooth-surfaced spheres, as described previously (Yamashita et al. 2011). First, we assessed the correlation between the size of the silica particles and their inflammatory effects. We incubated RAW264.7 cells with each type of silica particle and measured TNFα production in the culture supernatant, because TNFα is a crucial modulator of inflammation (Fig. 1b). Of the various silica particles, nSP30 and nSP70 induced the highest TNFα production, whereas the larger nSP300 and mSP1000 did not induce such inflammatory responses.

Next, we assessed the correlation between particle size and inflammatory effects in vivo (Fig. 1c, d). We intraperitoneally injected silica particles into BALB/c mice and counted the total number of live cells in the PCLF, because inflammation is known to induce local infiltration of various inflammatory cells (Busuttil et al. 2004). We found that nSP30 and nSP70 induced significant cell migration compared with PBS, whereas nSP300 and mSP1000 showed low cell accumulation (Fig. 1c). Furthermore, we analyzed cytokine and chemokine production in the PCLF by using a cytokine array system (Fig. 1d). nSP30 and nSP70 induced greater production of interleukin-5 (IL-5) and IL-6, macrophage chemoattractant protein-1 (MCP-1), and keratinocyte chemoattractant (KC) than did nSP300 and mSP1000, although TNFα production was not detected in the PCLF. These results indicate that the nanosilica particles possessed a more potent inflammatory effect than did the larger silica particles.

Involvement of mitogen-activated protein kinases in nanosilica particle-induced inflammation

Mitogen-activated protein kinases (MAPKs) are a family of proteins, including p38, ERK, and JNK, that play key roles in regulation of the production of proinflammatory mediators and in apoptotic cell death (Jeffrey et al. 2007). To investigate the mechanisms of nanosilica particle-induced inflammation, we treated RAW264.7 cells with silica particles and used Western blotting analysis to examine the activation of MAPKs (Fig. 2a–c). We detected the phosphorylation of p38, ERK, and JNK in nSP30- and nSP70-treated cells. In contrast, little or no phosphorylation of

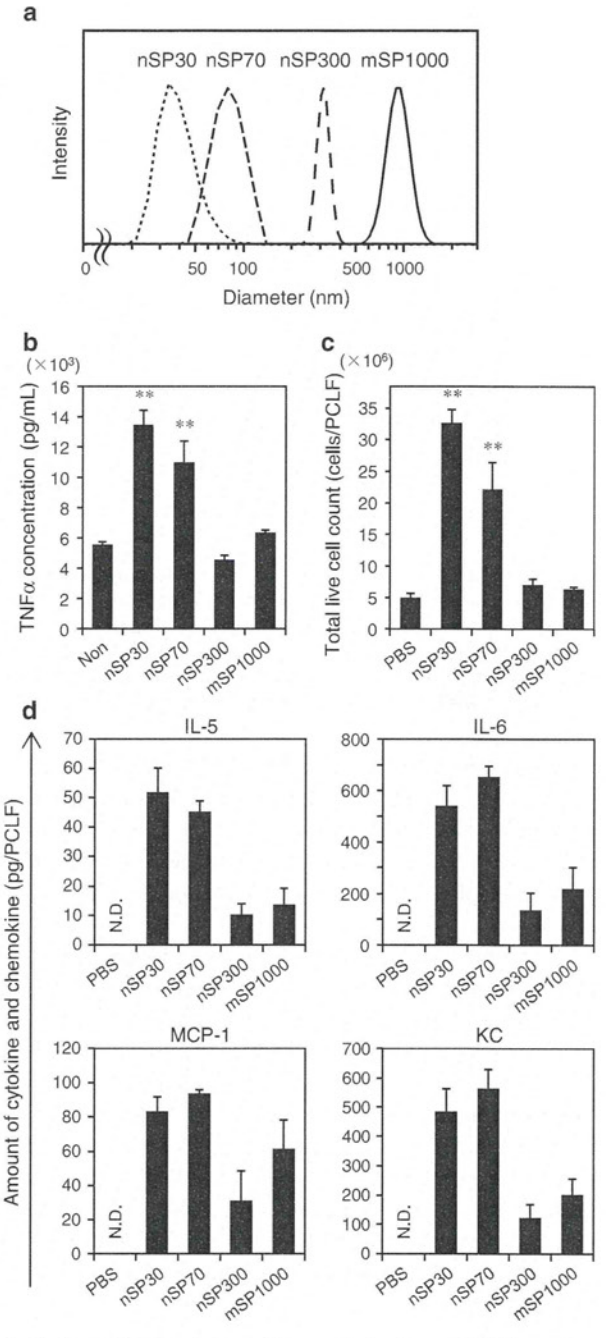

Fig. 1 Correlation between silica particle size and inflammatory effects in vitro and in vivo. **a** Size distribution of various sizes of silica particles was measured by a dynamic light-scattering method. **b** TNFα production levels in vitro. RAW264.7 cells were treated with each silica particle or no particles (Non) for 12 h, and then, TNFα production levels in the culture supernatants were measured. The data represent means ± SD ($n = 5$; $^{**}P < 0.01$ versus value for medium control, ANOVA). **c**, **d** In vivo inflammatory effects. BALB/c mice were intraperitoneally injected with PBS or each silica particle; then, **c** the total number of live cells in the PCLF was counted after 24 h, and **d** cytokine and chemokine production in the PCLF was measured after 2 h. *N.D.* not detected. Data represent means ± SEM ($n = 5$; $^{**}P < 0.01$ versus value for PBS control, ANOVA)

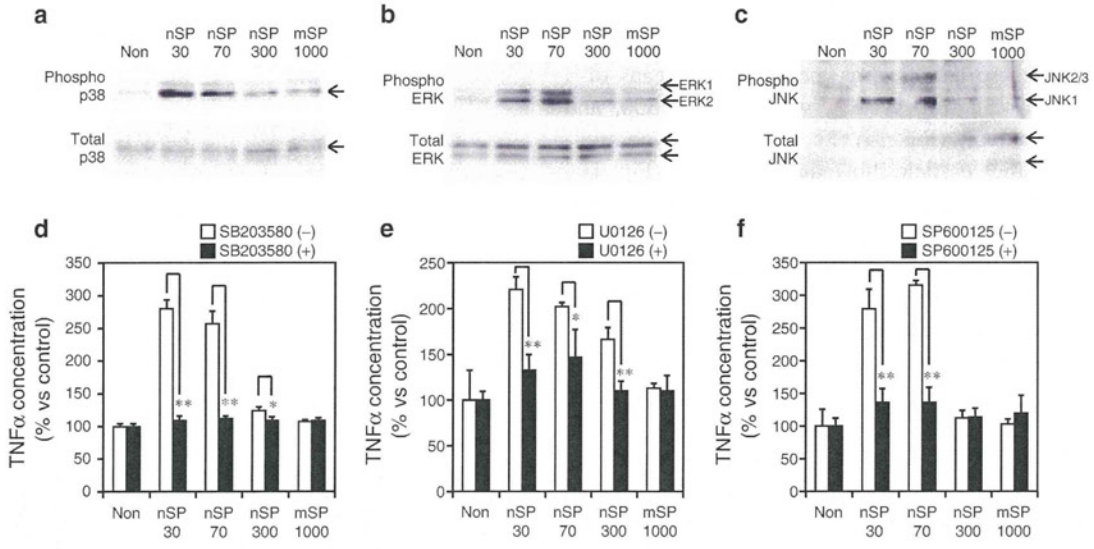

Fig. 2 Effects of silica particles on the activation of MAPKs. **a–c** Activation of MAPKs induced by silica particles. RAW264.7 cells were treated with silica particles of various sizes for 4 h. The whole-cell lysates were analyzed by Western blotting for phosphorylated and nonphosphorylated **a** p38, **b** ERK, and **c** JNK. **d–f** Association of MAPKs in silica particle-induced TNFα production. RAW264.7 cells, pretreated with inhibitors of **d** p38, **e** ERK, or **f** JNK were exposed to silica particles, and 4 h after the treatment, TNFα production in the culture supernatants was measured. Dimethyl sulfoxide (0.1%) was used as the control. Data represent means ± SD ($n = 5$; $^*P < 0.05$, $^{**}P < 0.01$ versus value for inhibitor [–] control within each treatment pair, t test)

MAPKs was detected in cells treated with nSP300 or mSP1000. No changes in the expression of nonphosphorylated p38, ERK, and JNK were observed in cells treated with silica particles. These results suggest that nanosilica particles might have induced inflammation via activation of MAPKs.

To confirm the importance of MAPKs in nanosilica particle-induced inflammation, we analyzed TNFα production in RAW264.7 cells treated with silica particles in the presence of an inhibitor of p38 (SB203580), ERK (U0126), or JNK (SP600125) (Fig. 2d–f). nSP30- and nSP70-induced TNFα production was almost completely suppressed by the inhibitors, indicating that nanosilica particle-induced TNFα production was mediated by MAPKs. Taken together, these results indicate that significant nanosilica particle-induced inflammation was mediated by the activation of MAPKs, whereas microsilica particles had little activation effect on MAPKs.

Involvement of the production of reactive oxygen species in nanosilica particle-induced inflammation

Intracellular reactive oxygen species (ROS) are reported to function as second messengers of inflammatory effects by activating multiple signaling pathways including a series of MAPKs (Bubici et al. 2006; Thannickal and Fanburg 2000). To investigate the involvement of ROS in nanosilica particle-induced TNFα production, we measured the TNFα concentrations induced by nSP30 and nSP70 in the presence BHA, a broad-spectrum ROS scavenger, or DPI, a specific inhibitor of NADPH oxidase, which is an important enzymatic producer of ROS (Morel et al. 1991). Both BHA and DPI significantly suppressed nanosilica particle-induced TNFα production (Fig. 3a, b), suggesting that nanosilica particle-induced production of ROS plays an important role in MAPK activation and subsequent inflammatory responses.

Suppression of inflammation by surface modification of nSP70

To investigate the influence of surface modification on nanosilica particle-induced inflammatory responses, we used nSP70 of which the surfaces had been modified with COOH groups (nSP70-C). We confirmed that nSP70-C were smooth-surfaced spherical particles by TEM as described previously (Yamashita et al. 2011). The mean secondary particle diameter of the nSP70-C was 70 nm, and the zeta potentials of nSP70 and nSP70-C were −53 and −76, respectively, indicating that surface modification changed the surface charge of the particles as described previously (Yamashita et al. 2011). We incubated RAW264.7 cells with nSP70 or nSP70-C for 12 h and then measured the TNFα concentrations. Whereas nSP70 induced high levels of TNFα production, nSP70-C induced low levels of TNFα production (Fig. 4a). Furthermore, we evaluated the inflammatory effects of nSP70 and nSP70-C in vivo. We intraperitoneally injected both types of particle separately into BALB/c mice

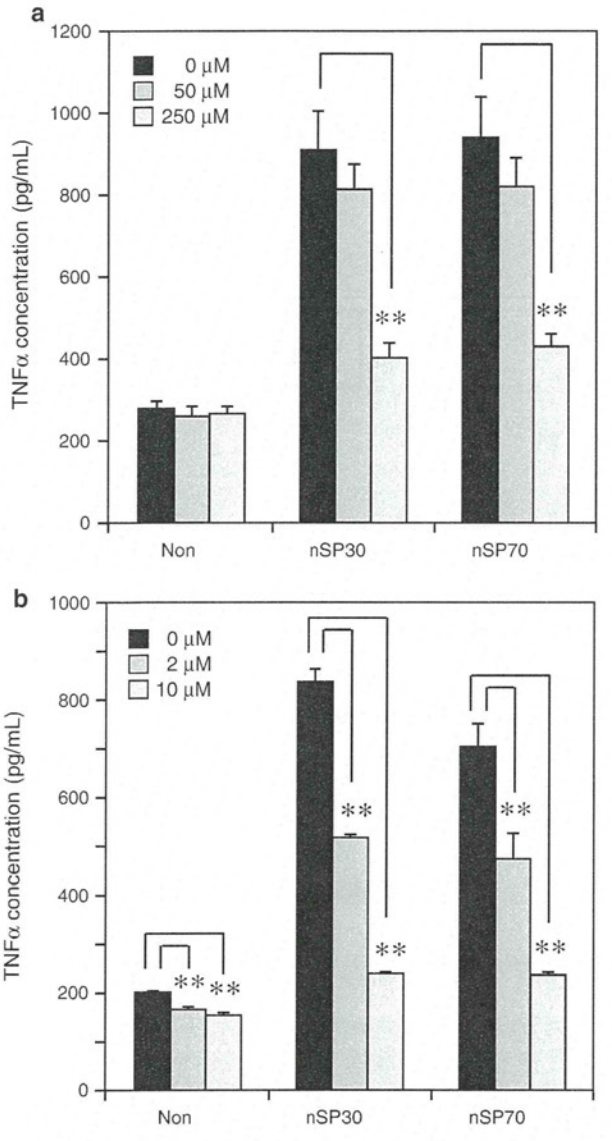

Fig. 3 Involvement of nanosilica particle-induced ROS production in TNFα production. RAW264.7 cells were treated with nSP30 or nSP70 for 4 h in the absence or presence of **a** BHA or **b** DPI at the indicated concentrations. TNFα production in the culture supernatants was measured. Data represent means ± SD ($n = 5$; $^{**}P < 0.01$ versus value for inhibitor [−] control within each treatment pair, t test)

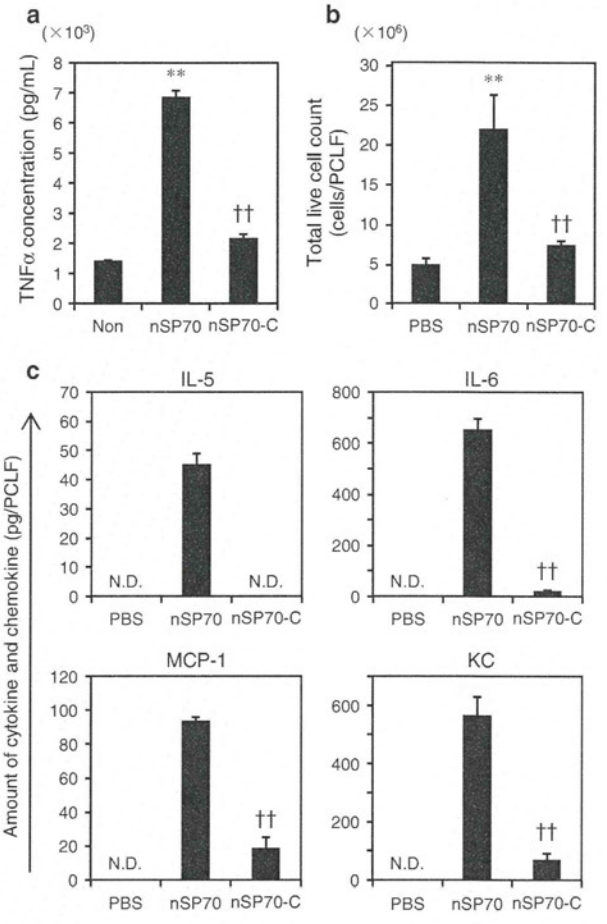

Fig. 4 Inflammatory responses induced by surface-modified nSP70. **a** TNFα production induced by nSP70 and nSP70-C. RAW264.7 cells were treated with nSP70 or nSP70-C for 12 h, and then, TNFα production in the culture supernatants was measured. Data represent means ± SD ($n = 5$; $^{**}P < 0.01$ versus value for medium control, $^{\dagger\dagger}P < 0.01$ versus value for nSP70, ANOVA). **b**, **c** In vivo inflammatory effects of nSP70 and nSP70-C. BALB/c mice were intraperitoneally injected with PBS or nSP70 or nSP70-C; **b** the total number of live cells in the PCLF was counted after 24 h, and **c** cytokine and chemokine production in the PCLF was measured after 2 h. *N.D.* not detected. Data represent means ± SEM ($n = 5$; $^{**}P < 0.01$ versus value for PBS control, $^{\dagger\dagger}P < 0.01$ versus value for nSP70, ANOVA)

and then counted the total number of live cells and measured the production of cytokines and chemokines in the PCLF. nSP70-C did not induce significant cell migration in treated mice, even though nSP70 induced strong inflammatory responses (Fig. 4b). In addition, cytokine and chemokine production in nSP70-C-treated mice was significantly lower than in nSP70-treated mice (Fig. 4c). We also confirmed that, in the 20-plex cytokine array system used in this study, there was no upregulation of cytokine and chemokine production in the nSP70-C-treated group (data not shown). These results indicate that nSP70 modified with COOH groups are unlikely to induce undesired inflammatory responses.

Suppression of MAPK activation by surface modification of nSP70

Through their phagocytic activity, macrophages play an important role in determining the biopersistence of foreign particles and initiating inflammatory responses, including cytokine production. Therefore, we speculated that the reduction of inflammatory responses by surface modification of nSP70 resulted from a difference in the particle

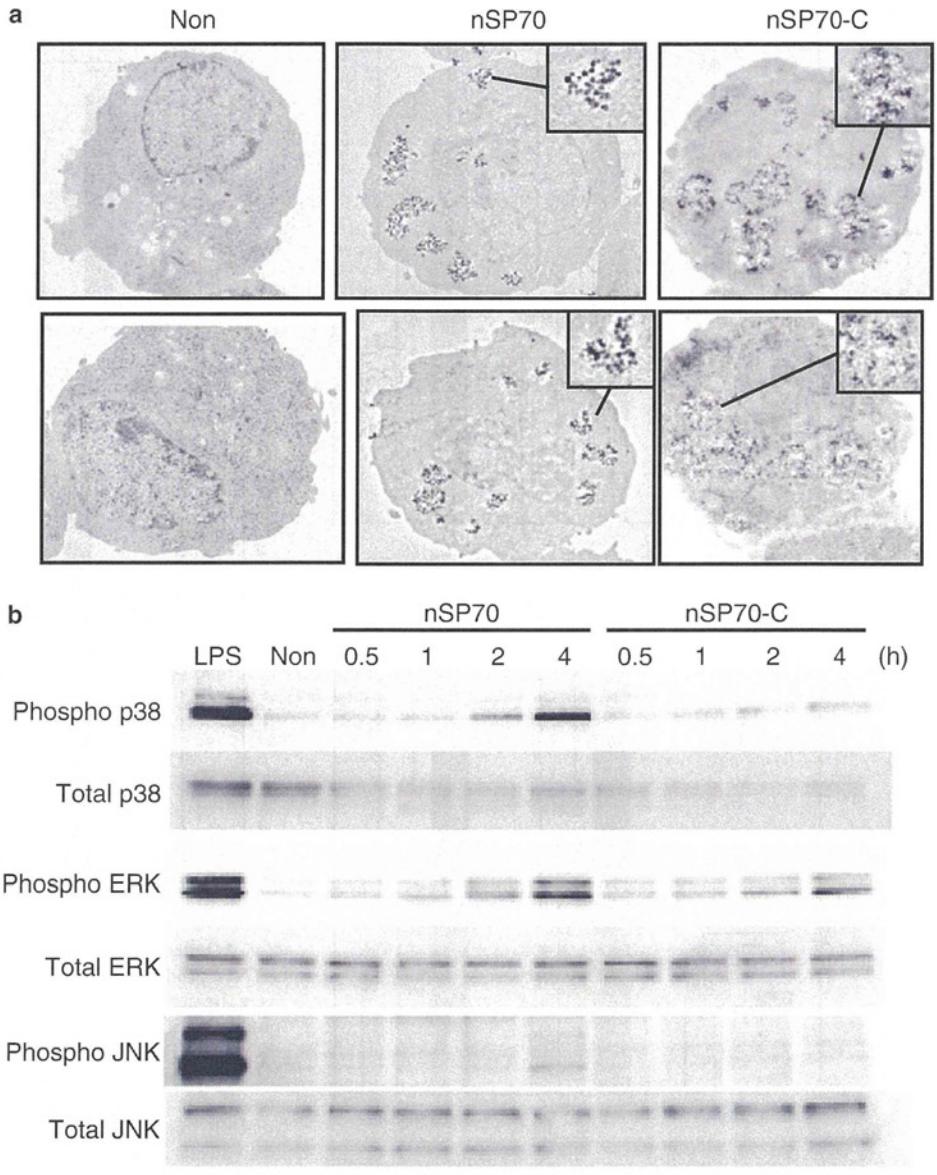

Fig. 5 Effects of surface modification of nSP70 on the MAPKs pathway. **a** TEM analysis of nSP70 and nSP70-C. RAW264.7 cells were treated with nSP70 or nSP70-C for 4 h. Cells were then observed by TEM. **b** MAPK activation induced by nSP70 or nSP70-C. RAW264.7 cells were treated with nSP70 or nSP70-C for the indicated times. The whole-cell lysate was analyzed by Western blotting for phosphorylated and nonphosphorylated p38, ERK, and JNK

uptake frequency between the modified and unmodified nSP70. TEM analysis of the uptake frequency of nSP70-C clearly showed that they were taken up by RAW264.7 cells as well as nSP70 (Fig. 5a). Therefore, we attributed the difference between the inflammatory effects of the modified and unmodified particles to a difference in signaling intensity after ingestion of the particles into the cells. To elucidate the mechanisms by which surface modification suppressed the inflammatory effect of nSP70, we examined the activity of MAPKs in RAW264.7 cells treated with modified or unmodified nSP70 (Fig. 5b). nSP70-C induced low MAPK activation compared with nSP70 4 h after the treatment, although there was no noticeable difference at the time point of 0.5, 1, and 2 h after the treatment. Taken together, our observations suggest that surface modification of nSP70 suppressed TNFα production by reducing nSP70-induced MAPK activation rather than by reducing cellular uptake frequency.

Cytotoxicity of silica particles

MAPKs are associated with cell growth, cell differentiation, and apoptotic cell death (Shiryaev and Moens 2010). Therefore, to investigate the influence of silica particle size on cytotoxicity, we treated RAW264.7 cells with silica particles of various sizes and examined the cell viability. nSP30 and nSP70 had significant cytotoxicity compared with the larger particles (nSP300 and mSP1000; Fig. 6a). To determine the impact of surface modification of the silica particles on cytotoxicity, we incubated RAW264.7

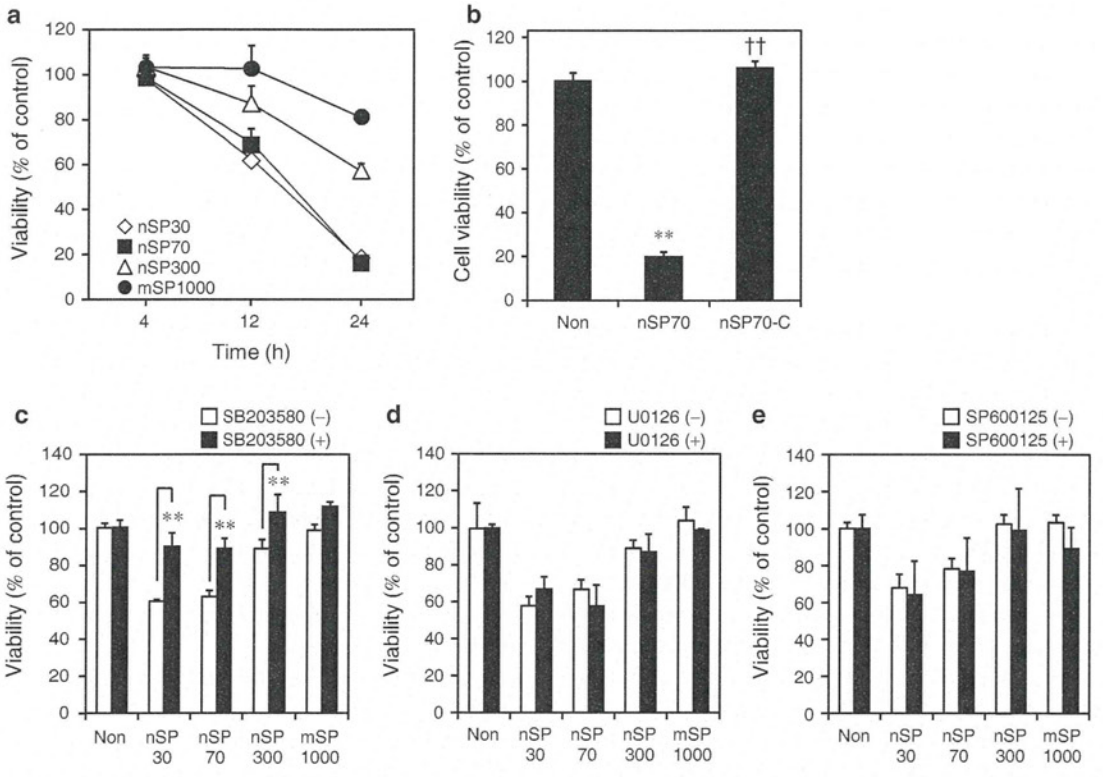

Fig. 6 Cytotoxicity induced by silica particles. **a** Cytotoxicity of silica particles. RAW264.7 cells were treated with silica particles of various sizes for the indicated time. Cell viability was assessed. Data represent means ± SD ($n = 5$). **b** Cytotoxicity of nSP70-C. RAW264.7 cells were treated with nSP70 or nSP70-C for 24 h. Cell viability was assessed. Data represent means ± SD ($n = 5$; $^{**}P < 0.01$ versus value for medium control, $^{\dagger\dagger}P < 0.01$ versus value for nSP70, ANOVA). **c–e** Association of MAPKs with silica particle-induced cell death. RAW264.7 cells pretreated with inhibitors of **c** p38 MAPK, **d** ERK, or **e** JNK were exposed to silica particles, and 12 h after the treatment, cell viability was assessed. Dimethyl sulfoxide (0.1%) was used as a control. Data represent means ± SD ($n = 5$; $^{**}P < 0.01$ versus value for inhibitor [–] control within each treatment pair, t test)

cells with nSP70 and nSP70-C and again evaluated the cell viability. nSP70-C showed no cytotoxicity, whereas nSP70 induced significant cell death (Fig. 6b). We speculated that nanosilica particle-induced cell death depended on MAPK signaling triggered by nanosilica particles. Therefore, to investigate the association of MAPKs and nanosilica particle-induced cell death, we treated RAW264.7 cells with silica particles in the presence or absence of an inhibitor of p38 (SB203580), ERK (U0126), or JNK (SP600125). The p38 inhibitor (SB203580) significantly suppressed the cytotoxicity of nanosilica particles (Fig. 6c–e), whereas the inhibitors of ERK (U0126) and JNK (SP600125) did not. These findings indicate that nanosilica particle-induced cell death depended in part on p38, but was independent of ERK and JNK.

Discussion

We elucidated the effects of particle size and surface modification on silica particle-induced inflammatory responses, with the goal of obtaining basic information for use in the development of safe and effective nanomaterials. First, we evaluated the association between the size of silica particles and their inflammatory effects. We focused on TNFα production, because TNFα stimulates the acute-phase reaction and is involved in systemic inflammation. Furthermore, recent reports have shown that TNFα plays a critical role in the pathogenesis of silicosis (Li et al. 2009). We showed that nSP30 and nSP70 induced significant TNFα production in vitro, whereas nSP300 and mSP1000 exhibited low levels of TNFα production (Fig. 1b). In addition, we demonstrated that the nSP30 and nSP70 induced higher in vivo inflammatory responses than did nSP300 and mSP1000 (Fig. 1c, d). Among the most important sources of cytokines against inhaled foreign particles are macrophages, which are widely known as the first line of defense against such particles (Hornung et al. 2008). We attributed nanosilica particle-induced cytokine production to the inflammatory signaling cascade triggered by ingestion of the nanosilica particles by macrophages. Consistent with our consideration, the results obtained by

other studies indicate that smaller titanium dioxide particles induce strong inflammatory responses than do larger particles (Sager et al. 2008). Therefore, we suggest that investigation of the mechanisms of nanosilica particle-induced inflammation is necessary for the development of safe and effective nanosilica particles. Although nSP30 and nSP70 induced in vitro inflammatory responses, we did not detect the production of TNFα in vivo, perhaps owing to the timing of our measurement of TNFα production (Savici et al. 1994).

We also investigated the mechanisms of the inflammatory effects of nanosilica particles on RAW264.7 macrophages. Intracellular ROS function as second messengers of inflammatory effects by activating multiple signal pathways including a series of MAPKs (Thannickal and Fanburg 2000). The activation of MAPKs leads to the induction of transcription factors for TNFα production, such as nuclear factor κB, activator protein 1, and activating transcription factor (Bubici et al. 2006). These transcription factors control the inducible expression of genes of which the products are part of the inflammatory response. In fact, Ke et al. (2006) reported that ROS play an essential role in crystalline silica-induced TNFα production. Here, we demonstrated that smaller nanosilica particles activated MAPKs more strongly than did larger silica particles, and furthermore, we showed that nanosilica particle-induced intracellular ROS were important factors in nanosilica particle-induced inflammatory responses of macrophages (Figs. 2, 3). Consistent with our results, the recent results of Liu et al. showed that exposure to silica nanoparticles causes the generation of ROS in endothelial cells, which in turn induces endothelial apoptosis via JNK/p53 and evokes the activation of nuclear factor κB pathways (Liu and Sun 2010). These observations collectively suggest that nSP30- and nSP70-induced intracellular ROS may participate in the activation of MAPKs and subsequent inflammatory responses.

In contrast, our previous data showed that, by activating the cytoplasmic NOD-like receptor family member NLRP3 inflammasome, mSP1000 induce higher IL-1β production than do nanosilica particles (Morishige et al. 2010a). These results indicate that there are differences in the intracellular behavior, signaling pathways, and cytokine production profiles induced by silica particles of various sizes. Although the detailed mechanisms by which nano- and microsilica particles induce different signaling cascades remain unclear, recent reports have shown that nanomaterials are introduced into the macrophages via foreign-recognizing scavenger receptors rather than via the traditional endocytosis pathway (Iyer et al. 1996; Thakur et al. 2009). In particular, scavenger receptor class A-mediated recognition and ingestion of nanomaterials reportedly induce cytotoxicity and cytokine production via activation of p38 (Hirano et al. 2008; Limmon et al. 2008). Therefore, we speculate that the difference between the inflammatory effects of nano- and microsilica particles was due to differences in the pathways by which they are recognized and ingested.

We also examined the effect of surface modification on the inflammatory effects of silica particles, because particle surface properties have been demonstrated to be important factors for the particles' biological effects (Albrecht et al. 2004; He et al. 2008; Morishige et al. 2010a; Yamashita et al. 2011). Interestingly, although unmodified nSP70 and surface-modified nSP70-C were equally taken up, we found that nSP70-C did not induce inflammatory responses in vitro or in vivo (Figs. 4, 5a). Furthermore, nSP70-C induced less MAPK activation (Fig. 5b). These results indicate that changes in surface properties, such as the surface charge, suppressed the inflammatory responses induced by nSP70. We previously demonstrated that surface modification of mSP1000 with functional groups, including COOH groups, efficiently decreases mSP1000-induced ROS production (Morishige et al. 2010a). Therefore, we speculate that the nSP70-C triggered less ROS production (which induces TNFα production) than did unmodified nSP70, although more precise investigation is needed. It has recently been shown that nanomaterials become coated with serum proteins and induce different cellular responses by binding to proteins (Lesniak et al. 2010; Lundqvist et al. 2008). In addition, different surface characteristics, such as surface charge and surface functional groups, are known to influence the binding affinities of proteins to nanomaterials (Lundqvist et al. 2008). Therefore, the differences in protein binding between nSP70 and nSP70-C might have given rise to differences in the nanomaterials' inflammatory responses.

In addition to cytokine production, cell death induced by nanosilica particles is also a critical obstacle to the safety and efficacy of nanosilica particles, because macrophages play a central role in the defense system of the host. Our data indicate that nSP30 and nSP70 induced significant cell death and that their cytotoxicity might be dependent on p38 but independent of ERK and JNK signaling (Fig. 6). These results indicate that nanosilica particle-induced cell death depended on activation of p38, whereas nanosilica particle-induced production of TNFα was not involved in cell death. Consistent with these considerations, nSP70-C, which induces less MAPKs activation, did not trigger cell death.

We demonstrated that nanosilica particles induced stronger inflammatory responses than did microsilica particles and that nanosilica particle-induced TNFα production was mediated by the activation of ROS and MAPKs. Furthermore, by surface modification with COOH groups, we suppressed nanosilica particle-induced inflammatory responses by inhibiting the activation of MAPKs. We expect

that further studies of the relationship between surface characteristics and biological effects will provide useful information for the development of safe and effective nanomaterials.

Acknowledgments This work was supported by the Ministry of Health, Labor, and Welfare in Japan; the Ministry of Education, Culture, Sports, Science, and Technology of Japan; and the Global COE Program "in silico medicine" at Osaka University.

Conflict of interest The authors declare that they have no competing interests.

References

Albrecht C, Schins RP, Hohr D, Becker A, Shi T, Knaapen AM et al (2004) Inflammatory time course after quartz instillation: role of tumor necrosis factor-alpha and particle surface. Am J Respir Cell Mol Biol 31:292–301

Bharali DJ, Klejbor I, Stachowiak EK, Dutta P, Roy I, Kaur N et al (2005) Organically modified silica nanoparticles: a nonviral vector for in vivo gene delivery and expression in the brain. Proc Natl Acad Sci USA 102:11539–11544

Bottini M, D'Annibale F, Magrini A, Cerignoli F, Arimura Y, Dawson MI et al (2007) Quantum dot-doped silica nanoparticles as probes for targeting of T-lymphocytes. Int J Nanomedicine 2:227–233

Bubici C, Papa S, Dean K, Franzoso G (2006) Mutual cross-talk between reactive oxygen species and nuclear factor-kappa B: molecular basis and biological significance. Oncogene 25: 6731–6748

Busuttil SJ, Ploplis VA, Castellino FJ, Tang L, Eaton JW, Plow EF (2004) A central role for plasminogen in the inflammatory response to biomaterials. J Thromb Haemost 2:1798–1805

Chen Z, Meng H, Xing G, Yuan H, Zhao F, Liu R et al (2008) Age-related differences in pulmonary and cardiovascular responses to SiO2 nanoparticle inhalation: nanotoxicity has susceptible population. Environ Sci Technol 42:8985–8992

Decuzzi P, Godin B, Tanaka T, Lee SY, Chiappini C, Liu X et al (2010) Size and shape effects in the biodistribution of intravascularly injected particles. J Control Release 141:320–327

Dostert C, Petrilli V, Van Bruggen R, Steele C, Mossman BT, Tschopp J (2008) Innate immune activation through Nalp3 inflammasome sensing of asbestos and silica. Science 320: 674–677

He X, Nie H, Wang K, Tan W, Wu X, Zhang P (2008) In vivo study of biodistribution and urinary excretion of surface-modified silica nanoparticles. Anal Chem 80:9597–9603

Hirano S, Kanno S, Furuyama A (2008) Multi-walled carbon nanotubes injure the plasma membrane of macrophages. Toxicol Appl Pharmacol 232:244–251

Hirsch LR, Stafford RJ, Bankson JA, Sershen SR, Rivera B, Price RE et al (2003) Nanoshell-mediated near-infrared thermal therapy of tumors under magnetic resonance guidance. Proc Natl Acad Sci USA 100:13549–13554

Hornung V, Bauernfeind F, Halle A, Samstad EO, Kono H, Rock KL et al (2008) Silica crystals and aluminum salts activate the NALP3 inflammasome through phagosomal destabilization. Nat Immunol 9:847–856

Huaux F (2007) New developments in the understanding of immunology in silicosis. Curr Opin Allergy Clin Immunol 7:168–173

Iyer R, Hamilton RF, Li L, Holian A (1996) Silica-induced apoptosis mediated via scavenger receptor in human alveolar macrophages. Toxicol Appl Pharmacol 141:84–92

Jeffrey KL, Camps M, Rommel C, Mackay CR (2007) Targeting dual-specificity phosphatases: manipulating MAP kinase signalling and immune responses. Nat Rev Drug Discov 6:391–403

Kagan VE, Bayir H, Shvedova AA (2005) Nanomedicine and nanotoxicology: two sides of the same coin. Nanomedicine 1:313–316

Ke Q, Li J, Ding J, Ding M, Wang L, Liu B et al (2006) Essential role of ROS-mediated NFAT activation in TNF-alpha induction by crystalline silica exposure. Am J Physiol Lung Cell Mol Physiol 291:L257–L264

Kops SK, Ratzlaff RE, Meade R, Iverson GM, Askenase PW (1986) Interaction of antigen-specific T cell factors with unique "receptors" on the surface of mast cells: demonstration in vitro by an indirect rosetting technique. J Immunol 136:4515–4524

Lesniak A, Campbell A, Monopoli MP, Lynch I, Salvati A, Dawson KA (2010) Serum heat inactivation affects protein corona composition and nanoparticle uptake. Biomaterials 31:9511–9518

Li X, Hu Y, Jin Z, Jiang H, Wen J (2009) Silica-induced TNF-alpha and TGF-beta1 expression in RAW264.7 cells are dependent on Src-ERK/AP-1 pathways. Toxicol Mech Methods 19:51–58

Limmon GV, Arredouani M, McCann KL, Corn Minor RA, Kobzik L, Imani F (2008) Scavenger receptor class-A is a novel cell surface receptor for double-stranded RNA. Faseb J 22:159–167

Liu X, Sun J (2010) Endothelial cells dysfunction induced by silica nanoparticles through oxidative stress via JNK/P53 and NF-kappaB pathways. Biomaterials 31:8198–8209

Lundqvist M, Stigler J, Elia G, Lynch I, Cedervall T, Dawson KA (2008) Nanoparticle size and surface properties determine the protein corona with possible implications for biological impacts. Proc Natl Acad Sci USA 105:14265–14270

Mantovani A, Allavena P, Sica A, Balkwill F (2008) Cancer-related inflammation. Nature 454:436–444

Mitchell LA, Lauer FT, Burchiel SW, McDonald JD (2009) Mechanisms for how inhaled multiwalled carbon nanotubes suppress systemic immune function in mice. Nat Nanotechnol 4:451–456

Morel F, Doussiere J, Vignais PV (1991) The superoxide-generating oxidase of phagocytic cells. Physiological, molecular and pathological aspects. Eur J Biochem 201:523–546

Morishige T, Yoshioka Y, Inakura H, Tanabe A, Yao X, Narimatsu S et al (2010a) The effect of surface modification of amorphous silica particles on NLRP3 inflammasome mediated IL-1beta production, ROS production and endosomal rupture. Biomaterials 31:6833–6842

Morishige T, Yoshioka Y, Tanabe A, Yao X, Tsunoda S, Tsutsumi Y et al (2010b) Titanium dioxide induces different levels of IL-1beta production dependent on its particle characteristics through caspase-1 activation mediated by reactive oxygen species and cathepsin B. Biochem Biophys Res Commun 392:160–165

Mossman BT, Churg A (1998) Mechanisms in the pathogenesis of asbestosis and silicosis. Am J Respir Crit Care Med 157: 1666–1680

Nel A, Xia T, Madler L, Li N (2006) Toxic potential of materials at the nanolevel. Science 311:622–627

Poland CA, Duffin R, Kinloch I, Maynard A, Wallace WA, Seaton A et al (2008) Carbon nanotubes introduced into the abdominal cavity of mice show asbestos-like pathogenicity in a pilot study. Nat Nanotechnol 3:423–428

Roy I, Ohulchanskyy TY, Bharali DJ, Pudavar HE, Mistretta RA, Kaur N et al (2005) Optical tracking of organically modified silica nanoparticles as DNA carriers: a nonviral, nanomedicine approach for gene delivery. Proc Natl Acad Sci USA 102:279–284

Sager TM, Kommineni C, Castranova V (2008) Pulmonary response to intratracheal instillation of ultrafine versus fine titanium dioxide: role of particle surface area. Part Fibre Toxicol 5:17

Savici D, He B, Geist LJ, Monick MM, Hunninghake GW (1994) Silica increases tumor necrosis factor (TNF) production, in part, by upregulating the TNF promoter. Exp Lung Res 20:613–625

Shiryaev A, Moens U (2010) Mitogen-activated protein kinase p38 and MK2, MK3 and MK5: menage a trois or menage a quatre? Cell Signal 22:1185–1192

Takagi A, Hirose A, Nishimura T, Fukumori N, Ogata A, Ohashi N et al (2008) Induction of mesothelioma in p53± mouse by intraperitoneal application of multi-wall carbon nanotube. J Toxicol Sci 33:105–116

Thakur SA, Hamilton R Jr, Pikkarainen T, Holian A (2009) Differential binding of inorganic particles to MARCO. Toxicol Sci 107:238–246

Thannickal VJ, Fanburg BL (2000) Reactive oxygen species in cell signaling. Am J Physiol Lung Cell Mol Physiol 279:L1005–L1028

Verraedt E, Pendela M, Adams E, Hoogmartens J, Martens JA (2009) Controlled release of chlorhexidine from amorphous microporous silica. J Control Release 142:47–52

Waters KM, Masiello LM, Zangar RC, Tarasevich BJ, Karin NJ, Quesenberry RD et al (2009) Macrophage responses to silica nanoparticles are highly conserved across particle sizes. Toxicol Sci 107:553–569

Yamashita K, Yoshioka Y, Higashisaka K, Morishita Y, Yoshida T, Fujimura M et al (2010) Carbon nanotubes elicit DNA damage and inflammatory response relative to their size and shape. Inflammation 33:276–280

Yamashita K, Yoshioka Y, Higashisaka K, Mimura K, Morishita Y, Nozaki M et al (2011) Silica and titanium dioxide nanoparticles cause pregnancy complications in mice. Nat Nanotechnol 6:321–328

Yang X, Liu J, He H, Zhou L, Gong C, Wang X et al (2010) SiO2 nanoparticles induce cytotoxicity and protein expression alteration in HaCaT cells. Part Fibre Toxicol 7:1

Biochemical and Biophysical Research Communications 420 (2012) 297–301

Contents lists available at SciVerse ScienceDirect

Biochemical and Biophysical Research Communications

journal homepage: www.elsevier.com/locate/ybbrc

Distribution and histologic effects of intravenously administered amorphous nanosilica particles in the testes of mice

Yuki Morishita [a], Yasuo Yoshioka [a,*], Hiroyoshi Satoh [a], Nao Nojiri [a], Kazuya Nagano [b], Yasuhiro Abe [c], Haruhiko Kamada [b,d], Shin-ichi Tsunoda [b,d], Hiromi Nabeshi [e], Tomoaki Yoshikawa [a], Yasuo Tsutsumi [a,b,d,*]

[a] Laboratory of Toxicology and Safety Science, Graduate School of Pharmaceutical Sciences, Osaka University, 1-6 Yamadaoka, Suita, Osaka 565-0871, Japan
[b] Laboratory of Biopharmaceutical Research, National Institute of Biomedical Innovation, 7-6-8 Saitoasagi, Ibaraki, Osaka 567-0085, Japan
[c] Cancer Biology Research Center, Sanford Research/USD, 2301 E. 60th Street N, Sioux Falls, SD 57104, USA
[d] The Center for Advanced Medical Engineering and Informatics, Osaka University, 1-6 Yamadaoka, Suita, Osaka 565-0871, Japan
[e] Division of Foods, National Institute of Health Sciences, 1-18-1, Kamiyoga, Setagaya-ku, Tokyo 158-8501, Japan

ARTICLE INFO

Article history:
Received 25 February 2012
Available online 6 March 2012

Keywords:
Biodistribution
Nanomaterials
Safety
Reproductive toxicity

ABSTRACT

Amorphous nanosilica particles (nSP) are being utilized in an increasing number of applications such as medicine, cosmetics, and foods. The reduction of the particle size to the nanoscale not only provides benefits to diverse scientific fields but also poses potential risks. Several reports have described the *in vivo* and *in vitro* toxicity of nSP, but few studies have examined their effects on the male reproductive system. The aim of this study was to evaluate the testicular distribution and histologic effects of systemically administered nSP. Mice were injected intravenously with nSP with diameters of 70 nm (nSP70) or conventional microsilica particles with diameters of 300 nm (nSP300) on two consecutive days. The intratesticular distribution of these particles 24 h after the second injection was analyzed by transmission electron microscopy. nSP70 were detected within sertoli cells and spermatocytes, including in the nuclei of spermatocytes. No nSP300 were observed in the testis. Next, mice were injected intravenously with 0.4 or 0.8 mg nSP70 every other day for a total of four administrations. Testes were harvested 48 h and 1 week after the last injection and stained with hematoxylin–eosin for histologic analysis. Histologic findings in the testes of nSP70-treated mice did not differ from those of control mice. Taken together, our results suggest that nSP70 can penetrate the blood-testis barrier and the nuclear membranes of spermatocytes without producing apparent testicular injury.

1. Introduction

With recent developments in nanotechnology, various kinds of nanomaterials have been designed and produced throughout the world. The small particle size and large surface area relative to volume enables nanomaterials to display a number of useful properties that are different from those of bulk materials, including high levels of electrical conductivity, tensile strength, electronic reactivity, and tissue permeability [1]. Because of these properties, nanomaterials have been widely used in consumer and industrial applications. In particular, amorphous nanosilica particles (nSP) possess a variety of unique properties, such as ease of synthesis, relatively low cost, and availability of sites for surface modifications [2,3], and nSP are increasingly being used for applications including cosmetics, foods, and drugs. However, several reports have shown that nSP might induce adverse effects such as pulmonary inflammation [4] and hemolysis [5]. Because nanomaterials have the potential to improve the quality of human life, it is essential to insure their safety and obtain the information necessary for designing safe nanomaterials. For the development of safe nanomaterials, we have been investigating the biologic distribution and biologic effects of nSP. We have already found that nSP can pass through biologic barriers, such as skin, the blood-brain barrier [6], and the blood-placental barrier [7] in mice. In addition, we found that nSP induces oxidative stress and DNA damage [8], allergic immune responses [9], and pregnancy complications [7] in mice, although the administration dose of nSP was higher than the dose of the human occupational exposure situation. Furthermore, we showed that surface modification of nSP with amine or carboxyl groups altered the intracellular distribution of the nSP and had an effect on cell proliferation [10], and suppressed toxic biologic effects of nSP such as pregnancy complications [7], indicating that surface modification prevented adverse effects of nSP and would be an approach to create safer nanomaterials.

* Corresponding authors. Address: Laboratory of Toxicology and Safety Science, Graduate School of Pharmaceutical Sciences, Osaka University, 1-6 Yamadaoka, Suita, Osaka 565-0871, Japan. Fax: +81 6 6879 8234.
E-mail addresses: yasuo@phs.osaka-u.ac.jp (Y. Yoshioka), ytsutsumi@phs.osaka-u.ac.jp (Y. Tsutsumi).

0006-291X/$ - see front matter © 2012 Elsevier Inc. All rights reserved.
doi:10.1016/j.bbrc.2012.02.153

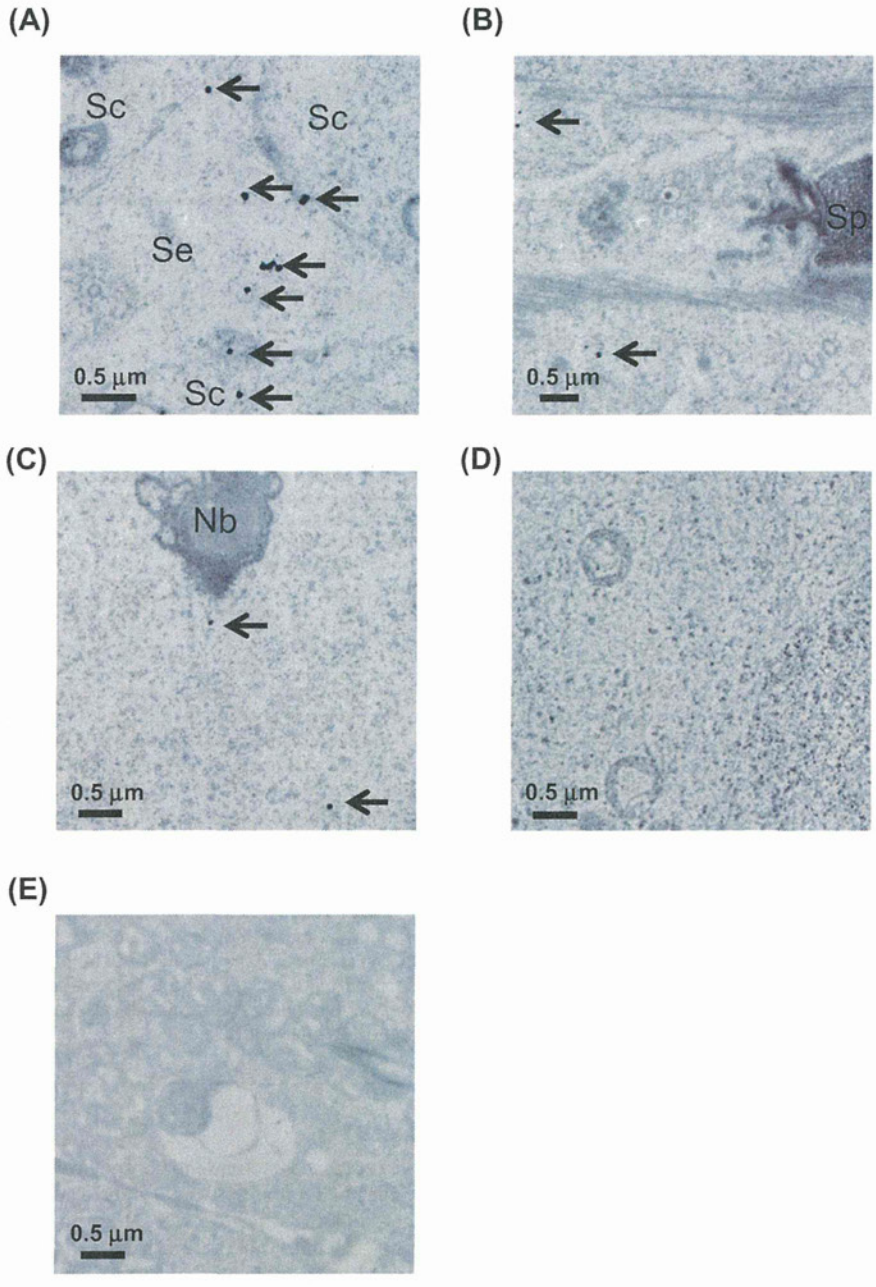

Fig. 1. Transmission electron micrographs of silica particles biodistribution in the testis. BALB/c mice were intravenously administered 0.8 mg of nSP70, nSP300, or saline on two consecutive days. Arrows indicate nSP70 present in Sertoli cells and spermatocytes (A), near sperm (B), and in the nucleus of a spermatocyte (C). No particles were observed in testes of nSP300 (D) or control mice (E). Sc: spermatocyte, Se: Sertoli cell, Sp: sperm, Nb: nuclear body.

Rates of male infertility continue to increase, and male infertility has been a difficult problem to solve [11]. Male infertility is for the most part caused by dysfunction of the testes. The testes are sensitive to many chemicals, such as endocrine disruptors [12], pesticides [13,14], and anticancer agents [15]. Therefore, to insure the reproductive safety of nSP, it is important to investigate their biologic effects on the testis. The toxicity of nanomaterials [16,17] and nanoparticle-rich diesel exhaust [18,19] to male reproductive functions has been investigated. For example, Bai et al. showed that multiwalled carbon nanotubes are distributed to the testis, where they induce reversible damage [17]. However, few studies have investigated the effect of nSP on the male reproductive system or the distribution of nanomaterials in testis and male germ cells, although information about the intra-testicular distribution would greatly help to elucidate the effect of nanomaterials on male reproductive systems.

Here, we qualitatively evaluated the intra-testicular distribution of nSP after intravenous administration in mice, including penetration of the blood-testis barrier and the distribution of nSP to germ cells. We also investigated the histologic effects of nSP on the testis.

2. Materials and methods

2.1. Silica particles

Amorphous silica particles (nSP70, 70-nm diameter; nSP300, 300-nm diameter) were purchased from Micromod Partikeltech-

nologie (Rostock-Warnemuende, Germany). The silica particles were used after 5 min of sonication (280 W output; Ultrasonic Cleaner, AS One, Osaka, Japan) and 1 min of vortexing.

2.2. Physicochemical examination of silica particles

Silica particles were diluted with PBS to 0.25 mg/mL (nSP70) or 0.5 mg/mL (nSP300), and the average particle size and zeta potential were measured using the Zetasizer Nano-ZS (Malvern Instruments Ltd., Worcestershire, UK). The mean size and the size distribution of silica particles were measured with the dynamic light scattering method. The zeta potential was measured by using laser Doppler electrophoresis.

2.3. Animals

BALB/c mice (male, 9 weeks old) were purchased from Japan SLC (Shizuoka, Japan). Mice were allowed to habituate to the animal room for 1 week prior to their use. The experimental protocols conformed to the ethical guidelines of Osaka University and the National Institute of Biomedical Innovation, Japan.

2.4. Transmission electron microscopy

BALB/c mice were injected intravenously through the tail vein with 100 μL (0.8 mg) of nSP70 or nSP300 on two consecutive days. The mice were anaesthetized and killed 24 h after the second injection, and the testes were fixed in 2.5% glutaraldehyde for 2 h. Small pieces of tissue collected from these samples were washed with phosphate buffer, postfixed in sodium cacodylate-buffered 1.5% osmium tetroxide for 60 min at 48 °C, dehydrated using a series of ethanol concentrations, and embedded in Epon resin. The samples were examined under a Hitachi electron microscope (H-7650; Hitachi, Tokyo, Japan).

2.5. Histology

Mice were given four doses of 100 μL (0.4 or 0.8 mg) nSP70 or saline (control), given intravenously through the tail vein every other day. Testes were collected 48 h or 1 week after the last administration. The testes were weighed and fixed in 10% neutral buffered formalin solution, dehydrated in a graded series of ethanol and xylene solutions, and embedded in paraffin. Sections were cut with a microtome, deparaffinized, rehydrated in a graded series of ethanols, and stained with hematoxylin and eosin.

2.6. Plasma biochemical analysis

Liver function was evaluated by measuring the plasma levels of alanine aminotransferase (ALT) and aspartate aminotransferase (AST). Nephrotoxicity was evaluated by measuring the plasma level of blood urea nitrogen (BUN). These markers were assayed by using a biochemical autoanalyzer, FUJI DRI-CHEM 7000 (Fujifilm, Tokyo, Japan).

2.7. Statistical analysis

All results are presented as means ± standard deviation (SD). Differences were compared by using Bonferroni's method after analysis of variance (ANOVA).

3. Results

Here we used nanosilica particles with diameters of 70 nm (nSP70) and conventional microsilica particles with diameters of 300 nm (nSP300). All of the silica particles were confirmed to be smooth-surfaced spheres, as we had previously described [6]. The hydrodynamic diameters of nSP70 and nSP300 were 77.0 and 269.3 nm, respectively, with zeta potentials of −21.6 and −31.3, respectively. The size distribution spectrum of each silica particle showed a single peak, and the hydrodynamic diameter corresponded almost precisely to the primary particle size for each sample, indicating that the silica used in this study were well-dispersed in solution (data not shown).

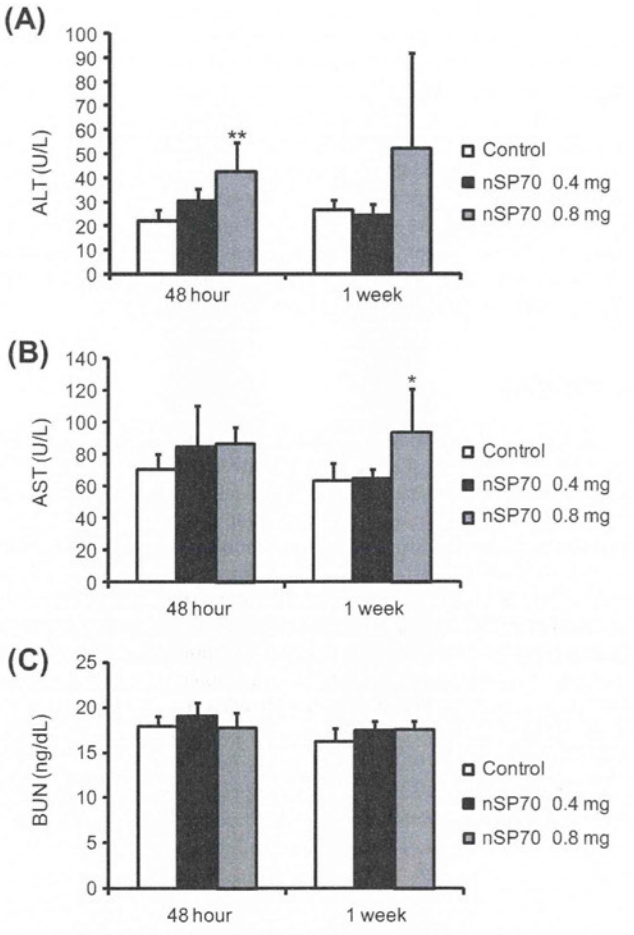

Fig. 2. Changes in liver and kidney damage markers in mouse plasma. Mice were given 0.4 or 0.8 mg nSP70 or saline intravenously every other day for a total of 4 doses. ALT (A), AST (B), and BUN (C) levels in plasma were evaluated 48 h and 1 week after the last injection. All data were presented as means ± SD ($n = 5$; $^{*}P < 0.05$, $^{**}P < 0.01$ versus value for control).

We had already found that nSP70 can enter the blood circulation after dermal administration [6]. To assess the biodistribution from the blood circulation, we used TEM to analyze the intratesticular distribution of each silica particle after intravenous injection. Dots with sharp outlines and appropriate sizes (70 nm for nSP70, 300 nm for nSP300) were identified as silica particles. The nSP70 were found in Sertoli cells, spermatocytes, and near sperm (Fig. 1A, B) and in both the cytoplasm and nuclei of spermatocytes (Fig. 1C). No particles were observed in testes of mice injected with nSP300 or of control mice (Fig. 1D, E). Although TEM provides only qualitative information, these results suggest that nSP70 were able to penetrate the blood-testis barrier and into the nuclei of spermatocytes, whereas nSP300 were not. The findings for nSP70, but not nSP300, are consistent with our previous results showing that nSP70 is distributed to placenta through blood-placental barrier [7].

Next, to evaluate whether nSP70 produce histologic effects on the testis, we administered four doses of 0.4 or 0.8 mg nSP70 intravenously every other day. The blood levels of ALT (Fig. 2A), ALT (Fig. 2B), and BUN (Fig. 2C) remained within the physiologic range, indicating that nSP70 did not induce liver and kidney damage at the administered doses, although some significant changes were observed in ALT and AST. Furthermore, the testes were weighed and analyzed histologically 48 h and 1 week after the last injection. Testis weights (Fig. 3A) and histologic findings (Fig. 3B) were not different in the testes of nSP70-treated mice and control mice. These results indicate that nSP70 can penetrate the blood-testis barrier without producing apparent testicular injury.

4. Discussion

In this study, we showed that nSP70, but not nSP300, were able to cross the blood-testis barrier. The limited histologic effects on the testes indicated that nSP70 may be actively transported across it without producing apparent testicular injury, although further investigation of the function of the blood-testis barrier in nSP70-treated mice is needed. By imaging fluorescently labeled nanoparticles, Kim et al. showed that 50-nm magnetic nanoparticles can also penetrate the mouse blood-testis barrier [20]. Therefore, the penetration of the blood-testis barrier is not specific to nSP. On the other hand, it is known that high-molecular-weight species (>500 Da) do not penetrate the blood-testis barrier by passive diffusion [21]. In fact, De Jong et al. showed with inductively coupled plasma mass spectrometry that gold nanoparticles larger than 50 nm were not distributed in the testis after intravenous administration [22]. Although differences in the dose or duration of administration and in the detection method might account for the different results, these findings suggest that the testicular distribution of nanomaterials might depend on the type of material. In this study, we evaluated the testicular distribution of nSP qualitatively, but testicular distribution of nanomaterials has also been evaluated quantitatively [17,23]. For example, Bai et al. measured the radioactivity of ^{64}Cu-labeled multiwalled carbon nanotubes in the testes of mice [17]. In future, the testicular distribution of nSP should also be quantitatively analyzed to further assess the reproductive safety of nSP.

We showed that nSP70 cause little overt testicular injury, although production of reproductive hormones and sperm function should also be examined. In contrast to our results with nSP70, intravenous administration of multiwalled carbon nanotubes do induce testis damage [17]. The total dose of nanomaterials that we administered in the current report was about five times higher than the total dose in the previous nanotube study. Therefore, we presume that nSP70 are safer to the testis than are multiwalled carbon nanotubes, although the duration of administration should also be taken into consideration.

Although nSP70 produced little testicular injury, the presence of nSP70 in the nuclei of spermatocytes suggests that DNA in the male germ line might be affected by nSP70. Abnormal DNA in the male germ line has been associated with an increased incidence of morbidity in the offspring [24], and paternal exposure to environmental factors has been suggested to influence biologic functions in offspring [25–27]. Therefore, the transgenerational effects of nSP as well as the direct effects on sperm should be evaluated in future studies.

In conclusion, this study showed that nSP70 can penetrate the blood-testis barrier without producing apparent testicular injury.

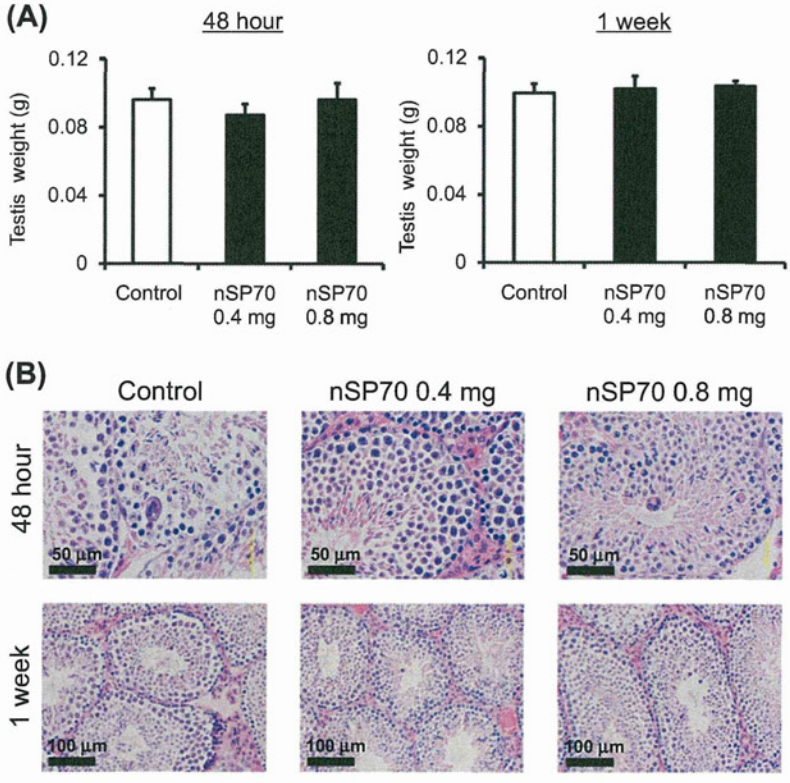

Fig. 3. Weight and pathological examination of the testis after four doses of nSP70. BALB/c mice were intravenously administered 0.4 or 0.8 mg of nSP70 or saline every other day for a total of four doses. Testes were weighed (A) and stained with hematoxylin–eosin (B) 48 h and 1 week after the last injection. Testis weight and histologic findings did not differ between nSP70-treated mice and control mice. All data were presented as means ± SD ($n = 5$).

Acknowledgments

This study was supported in part by Grants-in-Aid for Scientific Research from the Ministry of Education, Culture, Sports, Science and Technology of Japan (MEXT), and from the Japan Society for the Promotion of Science (JSPS); and by a the Knowledge Cluster Initiative (MEXT); by Health Labour Sciences Research Grants from the Ministry of Health, Labor and Welfare of Japan (MHLW); by a Global Environment Research Fund from Minister of the Environment; by Food Safety Commission (Cabinet Office); by The Cosmetology Research Foundation; by The Smoking Research Foundation; by The Takeda Science Foundation.

References

[1] O. Salata, Applications of nanoparticles in biology and medicine, J. Nanobiotechnol. 2 (2004) 3.
[2] T.K. Barik, B. Sahu, V. Swain, Nanosilica-from medicine to pest control, Parasitol Res. 103 (2008) 253–258.
[3] B. Fadeel, A.E. Garcia-Bennett, Better safe than sorry: understanding the toxicological properties of inorganic nanoparticles manufactured for biomedical applications, Adv. Drug Deliv. Rev. 62 (2010) 362–374.
[4] A.S. Yazdi, G. Guarda, N. Riteau, S.K. Drexler, A. Tardivel, I. Couillin, J. Tschopp, Nanoparticles activate the NLR pyrin domain containing 3 (Nlrp3) inflammasome and cause pulmonary inflammation through release of IL-1alpha and IL-1beta, Proc. Natl. Acad. Sci. USA 107 (2010) 19449–19454.
[5] T. Yu, A. Malugin, H. Ghandehari, Impact of silica nanoparticle design on cellular toxicity and hemolytic activity, ACS Nano 5 (2011) 5717–5728.
[6] H. Nabeshi, T. Yoshikawa, K. Matsuyama, Y. Nakazato, K. Matsuo, A. Arimori, M. Isobe, S. Tochigi, S. Kondoh, T. Hirai, T. Akase, T. Yamashita, K. Yamashita, T. Yoshida, K. Nagano, Y. Abe, Y. Yoshioka, H. Kamada, T. Imazawa, N. Itoh, S. Nakagawa, T. Mayumi, S. Tsunoda, Y. Tsutsumi, Systemic distribution, nuclear entry and cytotoxicity of amorphous nanosilica following topical application, Biomaterials 32 (2011) 2713–2724.
[7] K. Yamashita, Y. Yoshioka, K. Higashisaka, K. Mimura, Y. Morishita, M. Nozaki, T. Yoshida, T. Ogura, H. Nabeshi, K. Nagano, Y. Abe, H. Kamada, Y. Monobe, T. Imazawa, H. Aoshima, K. Shishido, Y. Kawai, T. Mayumi, S. Tsunoda, N. Itoh, T. Yoshikawa, I. Yanagihara, S. Saito, Y. Tsutsumi, Silica and titanium dioxide nanoparticles cause pregnancy complications in mice, Nat. Nanotechnol. 6 (2011) 321–328.
[8] H. Nabeshi, T. Yoshikawa, K. Matsuyama, Y. Nakazato, S. Tochigi, S. Kondoh, T. Hirai, T. Akase, K. Nagano, Y. Abe, Y. Yoshioka, H. Kamada, N. Itoh, S. Tsunoda, Y. Tsutsumi, Amorphous nanosilica induce endocytosis-dependent ROS generation and DNA damage in human keratinocytes, Part Fibre Toxicol. 8 (2011) 1.
[9] T. Yoshida, Y. Yoshioka, M. Fujimura, K. Yamashita, K. Higashisaka, Y. Morishita, H. Kayamuro, H. Nabeshi, K. Nagano, Y. Abe, H. Kamada, S. Tsunoda, N. Itoh, T. Yoshikawa, Y. Tsutsumi, Promotion of allergic immune responses by intranasally-administrated nanosilica particles in mice, Nanoscale Res. Lett. 6 (2011) 195.
[10] H. Nabeshi, T. Yoshikawa, A. Arimori, T. Yoshida, S. Tochigi, T. Hirai, T. Akase, K. Nagano, Y. Abe, H. Kamada, S. Tsunoda, N. Itoh, Y. Yoshioka, Y. Tsutsumi, Effect of surface properties of silica nanoparticles on their cytotoxicity and cellular distribution in murine macrophages, Nanoscale Res. Lett. 6 (2011) 93.
[11] S.S. Howards, Treatment of male infertility, N. Engl. J. Med. 332 (1995) 312–317.
[12] C.B. Herath, W. Jin, G. Watanabe, K. Arai, A.K. Suzuki, K. Taya, Adverse effects of environmental toxicants, octylphenol and bisphenol A, on male reproductive functions in pubertal rats, Endocrine 25 (2004) 163–172.
[13] S.Y. Zhang, Y. Ito, O. Yamanoshita, Y. Yanagiba, M. Kobayashi, K. Taya, C. Li, A. Okamura, M. Miyata, J. Ueyama, C.H. Lee, M. Kamijima, T. Nakajima, Permethrin may disrupt testosterone biosynthesis via mitochondrial membrane damage of Leydig cells in adult male mouse, Endocrinology 148 (2007) 3941–3949.
[14] A.T. Farag, A.H. Radwan, F. Sorour, A. El Okazy, S. El-Agamy el, K. El-Sebae Ael, Chlorpyrifos induced reproductive toxicity in male mice, Reprod. Toxicol. 29 (2010) 80–85.
[15] N. Elangovan, T.J. Chiou, W.F. Tzeng, S.T. Chu, Cyclophosphamide treatment causes impairment of sperm and its fertilizing ability in mice, Toxicology 222 (2006) 60–70.
[16] S. Yoshida, K. Hiyoshi, T. Ichinose, H. Takano, S. Oshio, I. Sugawara, K. Takeda, T. Shibamoto, Effect of nanoparticles on the male reproductive system of mice, Int. J. Androl. 32 (2009) 337–342.
[17] Y. Bai, Y. Zhang, J. Zhang, Q. Mu, W. Zhang, E.R. Butch, S.E. Snyder, B. Yan, Repeated administrations of carbon nanotubes in male mice cause reversible testis damage without affecting fertility, Nat. Nanotechnol. 5 (2010) 683–689.
[18] C. Li, S. Taneda, K. Taya, G. Watanabe, X. Li, Y. Fujitani, Y. Ito, T. Nakajima, A.K. Suzuki, Effects of inhaled nanoparticle-rich diesel exhaust on regulation of testicular function in adult male rats, Inhal. Toxicol. 21 (2009) 803–811.
[19] D.H. Ramdhan, Y. Ito, Y. Yanagiba, N. Yamagishi, Y. Hayashi, C. Li, S. Taneda, A.K. Suzuki, G. Watanabe, K. Taya, M. Kamijima, T. Nakajima, Nanoparticle-rich diesel exhaust may disrupt testosterone biosynthesis and metabolism via growth hormone, Toxicol. Lett. 191 (2009) 103–108.
[20] J.S. Kim, T.J. Yoon, K.N. Yu, B.G. Kim, S.J. Park, H.W. Kim, K.H. Lee, S.B. Park, J.K. Lee, M.H. Cho, Toxicity and tissue distribution of magnetic nanoparticles in mice, Toxicol. Sci. 89 (2006) 338–347.
[21] Y. Jin, I. Uchida, K. Eto, T. Kitano, S. Abe, Size-selective junctional barrier and Ca(2+)-independent cell adhesion in the testis of Cynops pyrrhogaster: expression and function of occludin, Mol. Reprod. Dev. 75 (2008) 202–216.
[22] W.H. De Jong, W.I. Hagens, P. Krystek, M.C. Burger, A.J. Sips, R.E. Geertsma, Particle size-dependent organ distribution of gold nanoparticles after intravenous administration, Biomaterials 29 (2008) 1912–1919.
[23] S.K. Balasubramanian, J. Jittiwat, J. Manikandan, C.N. Ong, L.E. Yu, W.Y. Ong, Biodistribution of gold nanoparticles and gene expression changes in the liver and spleen after intravenous administration in rats, Biomaterials 31 (2010) 2034–2042.
[24] R.J. Aitken, G.N. De Iuliis, R.I. McLachlan, Biologic and clinical significance of DNA damage in the male germ line, Int. J. Androl. 32 (2009) 46–56.
[25] M.D. Anway, A.S. Cupp, M. Uzumcu, M.K. Skinner, Epigenetic transgenerational actions of endocrine disruptors and male fertility, Science 308 (2005) 1466–1469.
[26] S.F. Ng, R.C. Lin, D.R. Laybutt, R. Barres, J.A. Owens, M.J. Morris, Chronic high-fat diet in fathers programs beta-cell dysfunction in female rat offspring, Nature 467 (2010) 963–966.
[27] B.R. Carone, L. Fauquier, N. Habib, J.M. Shea, C.E. Hart, R. Li, C. Bock, C. Li, H. Gu, P.D. Zamore, A. Meissner, Z. Weng, H.A. Hofmann, N. Friedman, O.J. Rando, Paternally induced transgenerational environmental reprogramming of metabolic gene expression in mammals, Cell 143 (2010) 1084–1096.

Arch Toxicol
DOI 10.1007/s00204-012-0823-5

INORGANIC COMPOUNDS

Suppression of nanosilica particle-induced inflammation by surface modification of the particles

Tomohiro Morishige · Yasuo Yoshioka · Hiroshi Inakura · Aya Tanabe · Shogo Narimatsu · Xinglei Yao · Youko Monobe · Takayoshi Imazawa · Shin-ichi Tsunoda · Yasuo Tsutsumi · Yohei Mukai · Naoki Okada · Shinsaku Nakagawa

Received: 17 August 2011 / Accepted: 27 February 2012

Abstract It has gradually become evident that nanomaterials, which are widely used in cosmetics, foods, and medicinal products, could induce substantial inflammation. However, the roles played by the physical characteristics of nanomaterials in inflammatory responses have not been elucidated. Here, we examined how particle size and surface modification influenced the inflammatory effects of nanosilica particles, and we investigated the mechanisms by which the particles induced inflammation. We compared the inflammatory effects of silica particles with diameters of 30–1,000 nm in vitro and in vivo. In macrophages in vitro, 30- and 70-nm nanosilica particles (nSP30 and nSP70) induced higher production of tumor necrosis factor-α (TNFα) than did larger particles. In addition, intraperitoneal injection of nSP30 and nSP70 induced stronger inflammatory responses involving cytokine production than did larger particles in mice. nSP70-induced TNFα production in macrophage depended on the production of reactive oxygen species and the activation of mitogen-activated protein kinases (MAPKs). Furthermore, nSP70-induced inflammatory responses were dramatically suppressed by surface modification of the particles with carboxyl groups in vitro and in vivo; the mechanism of the suppression involved reduction in MAPK activation. These results provide basic information that will be useful for the development of safe nanomaterials.

Keywords Inflammation · Macrophage · Nanoparticle · Silica · Surface modification

Abbreviations

BHA	Butylated hydroxyanisole
DPI	Diphenyleneiodonium chloride
ELISA	Enzyme-linked immunosorbent assay
ERK	Extracellular signal-regulated kinase
IL	Interleukin
JNK	C-jun N-terminal kinase
KC	Keratinocyte chemoattractant
MAPKs	Mitogen-activated protein kinases
MCP-1	Macrophage chemoattractant protein-1
PBS	Phosphate-buffered saline
PCLF	Peritoneal cavity lavage fluid
ROS	Reactive oxygen species
TEM	Transmission electron microscopy
TNFα	Tumor necrosis factor-α

T. Morishige · H. Inakura · A. Tanabe · S. Narimatsu · X. Yao · Y. Mukai · N. Okada · S. Nakagawa (✉)
Laboratory of Biotechnology and Therapeutics, Graduate School of Pharmaceutical Sciences, Osaka University, 1-6 Yamadaoka, Suita, Osaka 565-0871, Japan
e-mail: nakagawa@phs.osaka-u.ac.jp

Y. Yoshioka · S. Tsunoda · Y. Tsutsumi · S. Nakagawa
The Center for Advanced Medical Engineering and Informatics, Osaka University, 1-6 Yamadaoka, Suita, Osaka 565-0871, Japan

Y. Yoshioka · S. Tsunoda · Y. Tsutsumi
Laboratory of Biopharmaceutical Research, National Institute of Biomedical Innovation, Osaka 567-0085, Japan

X. Yao
Institute of Pharmaceutics, Zhejiang University, 388 Yuhangtang Road, Hangzhou 310058, China

Y. Monobe · T. Imazawa
Laboratory of Common Apparatus, Division of Biomedical Research, National Institute of Biomedical Innovation, Osaka 567-0085, Japan

Y. Tsutsumi
Laboratory of Toxicology and Safety Science, Graduate School of Pharmaceutical Sciences, Osaka University, Osaka 565-0871, Japan

Published online: 15 March 2012

Introduction

Many nanomaterials with innovative functions have been developed. For example, titanium dioxide nanoparticles, carbon nanotubes, and nanosilica particles have already been used commercially in electronics, medicine, cosmetics, and foods. Amorphous (noncrystalline) nanosilica particles with extraordinary properties can be synthesized by straightforward methods and are relatively inexpensive, and surface modification of the particles is easy to accomplish. In addition, they are usually considered to have low toxicity, in contrast to crystalline silica, which can cause silicosis and some forms of lung cancer (Huaux 2007; Mossman and Churg 1998). Therefore, nanosilica particles have been used for many applications, including cosmetics, foods, medical diagnosis, and drug delivery (Bharali et al. 2005; Bottini et al. 2007; Hirsch et al. 2003; Roy et al. 2005; Verraedt et al. 2009).

However, the increasing use of nanomaterials has raised public concern about their safety (Kagan et al. 2005; Nel et al. 2006). Carbon nanotubes have been reported to induce mesothelioma-like lesions in mice upon injection (Poland et al. 2008; Takagi et al. 2008), in a similar manner to crocidolite asbestos, and to suppress the immune system and damage DNA (Mitchell et al. 2009; Yamashita et al. 2010). Furthermore, nanosilica particles have been reported to induce oxidative stress, genotoxicity, and inflammation in vitro and in vivo (Chen et al. 2008; Liu and Sun 2010; Yang et al. 2010). Because inflammation has been implicated as the key factor in the development of chronic obstructive pulmonary disease, fibrosis, and carcinogenesis (Dostert et al. 2008; Mantovani et al. 2008), the need to investigate the inflammatory effects of nanosilica particles and ensure their safety is urgent.

Our group and others have recently reported that the characteristics of particles, including size and surface properties, are important factors in pathologic alterations and cellular responses (Albrecht et al. 2004; He et al. 2008; Morishige et al. 2010a, b; Waters et al. 2009; Yamashita et al. 2011). For example, we showed that administration of nanosilica particles into pregnant mice induces pregnancy complications, whereas microsilica particles have no effect (Yamashita et al. 2011). Furthermore, Decuzzi et al. (2010) demonstrated that the biodistribution of silica particles depends on particle size. However, only a few studies have assessed the roles of the physical characteristics of nanomaterials in relation to the inflammatory responses they induce. Therefore, the relationship between nanoparticle characteristics and biological effects, including inflammatory effects, and the precise mechanisms of these effects must be investigated. In addition, the results of such investigations should be used to develop a methodology for decreasing the adverse biological effects of nanomaterials.

In this study, we evaluated the correlation between inflammatory effects and the size and surface modification of silica particles. Furthermore, we investigated the mechanisms of the inflammatory responses induced by nanosilica particles.

Materials and methods

Materials and reagents

Unmodified amorphous silica particles with diameters of 30, 70, 300, or 1,000 nm (designated nSP30, nSP70, nSP300, and mSP1000, respectively) and nSP70 with surface carboxyl groups (nSP70-C) were purchased from Micromod Partikeltechnologie (Rostock/Warnemünde, Germany). Butylated hydroxyanisole (BHA) and diphenyleneiodonium chloride (DPI) were purchased from Sigma-Aldrich (St. Louis, MO). Rabbit polyclonal anti-phospho-p38 antibody (sc-17852-R) and mouse monoclonal anti-β-actin antibody (sc-47778; clone C4) were purchased from Santa Cruz Biotechnology (Santa Cruz, CA). Rabbit polyclonal anti-extracellular signal-regulated kinase (ERK)1/2 antibody (#9102), rabbit polyclonal anti-c-jun N-terminal kinase (JNK) antibody (#9252), rabbit monoclonal anti-phospho-JNK antibody (#4671; clone 98F2), and goat anti-rabbit peroxidase-conjugated antibody (#7074) were purchased from Cell Signaling Technology (Danvers, MA). Rabbit monoclonal anti-phospho-ERK1/2 antibody (MAB1018; clone269434) was obtained from R&D Systems (Minneapolis, MN). Rabbit polyclonal anti-p38 antibody (ab47437) was purchased from Abcam (Tokyo, Japan). Goat anti-mouse peroxidase-conjugated antibody was purchased from SouthernBiotech (Birmingham, AL). p38 inhibitor SB203580, ERK inhibitor U0126, and JNK inhibitor SP600125 were obtained from Merck (Darmstadt, Germany).

Cells and mice

RAW264.7 (mouse monocyte/macrophage cell line) cells were obtained from the American Type Culture Collection (Manassas, VA) and cultured at 37°C in Dulbecco's modified Eagle's medium (Wako Pure Chemical Industries, Osaka, Japan) supplemented with 10% fetal bovine serum and antibiotics. Female BALB/c mice were purchased from Nippon SLC (Shizuoka, Japan) and used at 8 weeks of age. All the animal experimental procedures were performed in accordance with Osaka University's guidelines for the welfare of animals.